Supporting Information

The Nature of Non-FRET Photoluminescence Quenching in Nanoassemblies from Semiconductor Quantum Dots and Dye Molecules

Aleksander P. Stupak[a], Thomas Blaudeck[b#], Eduard I. Zenkevich[c], Stefan Krause[b,&], and Christian von Borczyskowski[b]*

[a]B. I. Stepanov Institute of Physics, National Academy of Sciences of Belarus, Prospect Nezavisimosti 70, 220072 Minsk, Belarus

[b]Institute of Physics and Center for Nanostructured Materials and Analytics, Technische Universität Chemnitz, Reichenhainer Str. 70, D-09107 Chemnitz, Germany

[c]Department of Information Technologies and Robotics, National Technical University of Belarus, Prospect Nezavisimosti 65, 220013 Minsk, Belarus

[#]Present address: Department of Electrical Engineering and Information Technology, Center for Microtechnologies, Technische Universität Chemnitz, Reichenhainer Str. 70, D-09107 Chemnitz, Germany

[&]Present address: Department of Chemistry, University of Copenhagen, Universitätsparken 5, 2100 Copenhagen, Denmark

[*]Corresponding Author: C. von Borczyskowski: **borczyskowski@physik.tu-chemnitz.de**

S1 Analysis of *QD PL Intensity Quenching*

For the analysis of the PL intensity quenching as a function of the number of porphyrin molecules per QD, the well-known Stern-Volmer formalism [1] was modified. In our more generalized approach, the luminescence quenching can be described by

$$\frac{I_0}{I(x)} = 1 + \int_0^{\infty} K\ (x) \cdot dx\,. \qquad \text{(S1)}$$

$I(x)$ and I_0 represent the integrated PL intensity of the QD in presence (I(x)) and absence (I_0) of the chromophores, respectively. In this approach, the Stern-Volmer function $K(x)$ depends explicitly on the ratio x of (m-Pyr)$_4$H$_2$P to QD molar concentrations and can be expressed by the first derivative $K_{SV}^{D}(x$ of the experimental data plotted in conventional Stern-Volmer representation [2, 3]. “D” stands for the QD as a possible donor in FRET related processes. Using this approach, the corresponding K_{SV}^{A} values have been derived from the acceptor A (H$_2$P) fluorescence enhancement measurements at every titration step.

References

[1] B. Valeur. *Wiley-VCH* (2002) Weinheim.

[2] T. Blaudeck, E. Zenkevich, M. Abdel-Mottaleb, K. Szwaykowska, D. Kowerko, F. Cichos, C. von Borczyskowski. Formation Principles and Ligand Dynamics for Nanoassemblies of CdSe Quantum Dots and Functionalized Dye Molecules. *ChemPhysChem* (2012) **13** 959-972.
[3] T. Blaudeck, E. Zenkevich, F. Cichos, C. von Borczyskowski. Probing Wave Functions at Semiconductor Quantum Dot Surfaces by Non-FRET Photoluminescence Quenching. *J. Phys. Chem. C* (2008) **112** 20251–20257.

S2 QD PL Donor Quenching and Acceptor Fluorescence Enhancement Efficiencies

Experimental QD PL quenching efficiencies $\Phi_{quench} = 1 - I(x)/I(0)$ are obtained for every QD at every step of titration by (m-Pyr)$_4$H$_2$P in toluene at ambient temperature, where $I(0)$ is the integrated intensity of the QD PL band without porphyrin, $I(x)$ is the corresponding intensity at a given molar ratio x.

Porphyrin fluorescence enhancement efficiencies Φ_{FRET} caused by FRET have been obtained by two alternative approaches. In the first method, at every titration step, FRET efficiencies Φ_{FRET} have been calculated from the direct measurements of the corresponding intensities in fluorescence excitation spectra and optical densities (OD) in absorption spectra of QD-porphyrin mixture using the equation [1, 2]

$$\Phi_{\mathrm{FRET}} = \left[\frac{\mathrm{I_{DA}}(\lambda_{\mathrm{ex}} = 465\mathrm{nm}) - \mathrm{I_A}(\lambda_{\mathrm{ex}} = 465\mathrm{nm})}{\mathrm{I_A}(\lambda_{\mathrm{ex}} = 590\mathrm{nm})}\right] : \left[\frac{\mathrm{OD_{DA}}(465\mathrm{nm}) - \mathrm{OD_A}(465\mathrm{nm})}{\mathrm{OD_A}(590\mathrm{nm})}\right]. \quad \text{(S2)}$$

Here, I_{DA} corresponds to the porphyrin fluorescence intensity at λ_{em} = 651 nm for "QD-porphyrin" nanoassemblies , whereas I_A is the fluorescence intensity of porphyrin at the same molar ratio at two different excitation wavelengths (465 and 590 nm). *OD* are the corresponding optical densities of the solution at a given molar ratio x. The difference $I_{DA}(\lambda_{ex} = 465nm) - I_A(\lambda_{ex} = 465nm)$ reflects the increase of the acceptor emission intensity due to FRET. λ_{ex} = 590 nm corresponds to the wavelength, where the absorption of QD is at minimum. Additionally, the corresponding porphyrin fluorescence intensity has to be corrected for the residual QD PL at 651 nm as a function of x assuming a linear superposition of PL signals from QD and porphyrin.

FRET efficiencies have been in most of our experiments evaluated on the basis of the measured porphyrin fluorescence intensity using an alternative approach described in [1, 3-6] according to

$$\Phi_{FRET} = \frac{\varepsilon_A(\lambda_{exc}) \cdot F_{AD} - F_A}{\varepsilon_D(\lambda_{exc}) \cdot F_A \cdot n} \qquad \text{(S3)}$$

where F_{AD} corresponds to the acceptor (A, porphyrin) fluorescence intensity in the presence of a QD donor D and measured at λ_{em} = 651 nm (maximum of Q(0,0) band of porphyrin fluorescence) while exciting at the strong donor absorption λ_{exc} = 465 nm. F_A corresponds to

emission under the same λ_{em} and λ_{exc} conditions in the absence of the QD (donor). n is the number of A-molecules per D-QD, ε_A and ε_D are molar extinction coefficients of A and D, respectively, at the excitation wavelength λ_{ex}.

References

[1] E. Zenkevich, F. Cichos, A. Shulga, E. Petrov, T. Blaudeck, C. von Borczyskowski. Nanoassemblies designed from semiconductor quantum dots and molecular arrays. *J. Phys. Chem. B* (2005) **109** 8679-8692.

[2] E.I. Zenkevich, E.I. Sagun, V.N. Knyukshto, A.S. Stasheuski, V.A. Galievsky, A.P. Stupak, T. Blaudeck, C. von Borczyskowski. Quantitative Analysis of Singlet Oxygen ($^1O_2$) Generation via Energy Transfer in Bioconjugates Based on Semiconductor Quantum Dots and Porphyrin Ligands. *J. Phys. Chem. C* (2011) **115** 21535-21545.

[3] E. Zenkevich, A. Shulga, A. Chernook, Gurinovich. Migration of energy of electronic excitation in the chemical dimers of the cyclopentaneporphyrins. *J. Appl. Spectr*. (1986) **45** 984-991.

[4] A. Clapp, I. Medintz, J. Mauro, B. Fisher, M. Bawendi, H. Mattoussi. Fluorescence resonance energy transfer between quantum dot donors and dye-labeled protein acceptors. *J. Am. Chem. Soc.* (2004) **126** 301-310.

[5] K. E. Knowles, D. B. Tice, E. A. McArthur, G. C. Solomon, E. A. Weiss, E. A. Chemical control of the photoluminescence of CdSe quantum dot-organic complexes with a series of para-substituted aniline ligands. *J. Am. Chem. Soc*. (2010) **132** 1041–1050.

[6] J. R. Lakowicz. Principles of Fluorescence Spectroscopy. *Springer* (2006) New York.

S3 Influence of Dyes upon QD PL decay kinetics

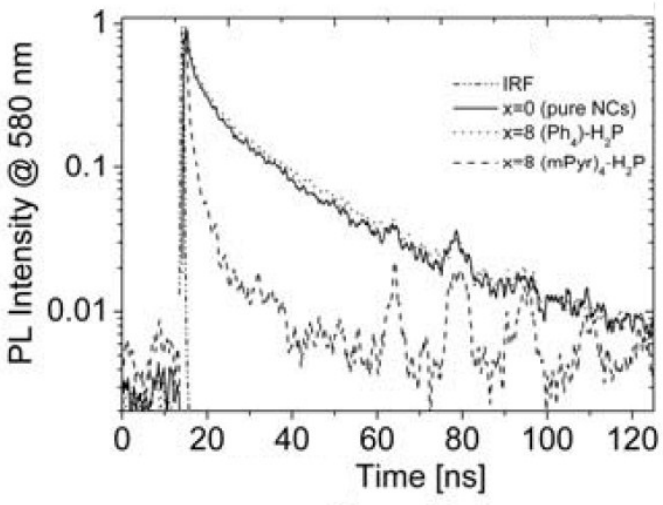

Figure S1 PL decay of CdSe(SO) (TOPO capped in toluene at RT) at x = 0 (full line) and x = 8 (broken line) detected at 580 nm. Titration with non-complexing H_2P-$(Ph)_4$ (TPP; dotted line) follows exactly the decay for x = 0. The experimental response function IRF is also shown.

S4 Comparison of Static and Dynamic PL Quenching

Both approaches, the quenching of the static PL intensity $I(x)$ and the shortening of PL decay times $\tau(x)$ can be treated within the Stern-Volmer approximation at a relative (dye) quencher concentration x according to [1, 2]

$$\frac{I_0}{I(x)} = 1 + K_{SV}{}^{D} \cdot x = 1 + k_q \cdot < \tau_0 > \cdot x = \frac{< \tau_0 >}{< \tau(x) >}, \qquad \text{(S4)}$$

where I_0 and $<\tau_0>$ apply at $x = 0$. Since the PL decay has to be fitted by 3 exponential decay terms we determined $<\tau_0>$ and $<\tau(x)>$ according to Equ. 4 in the manuscript. $K_{SV}{}^{D}(x)$ corresponds to the (differential) Stern-Volmer constant and k_q to the quenching rate with $\tau_0 k_q = K_{SV}{}^{D}(x)$ [3]. Equ. (S4) is only valid in case there is only one unique quenching mechanism. Figure S2 shows that the quenching of the donor (QD) PL follows $K_{SV}{}^{D}(I(x)) \approx 1.25\ K_{SV}{}^{D}(\tau(x))$ (assuming linear relationships across the given molar ratio range). Taking into account that experiments have been performed on different samples both $K_{SV}(x)$ values are in reasonable agreement with each other though Stern-Volmer constants are decreasing with increasing x (see Figure 1 in the main text of the paper) [3].

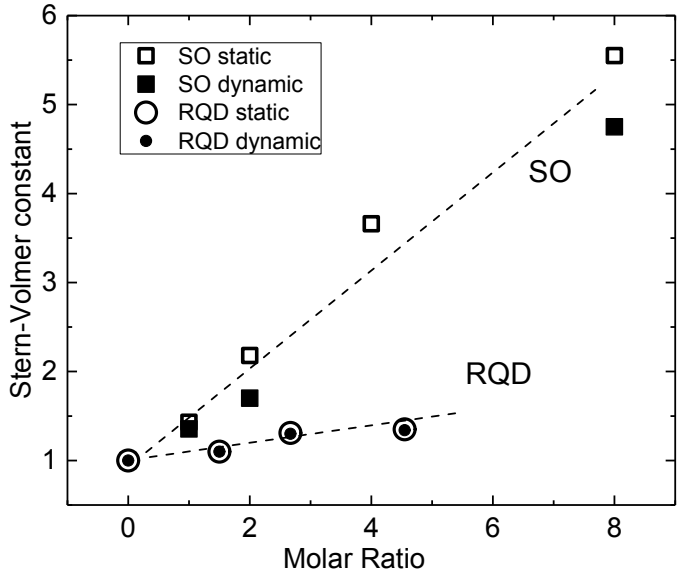

Figure S2 Stern-Volmer plot of the PL intensities I for CdSe(SO)-H_2P (open squares) or CdSe/ZnS(RQD)-H_2P (open circles) and related average lifetimes $<\tau(x)>$ (filled squares and filled circles, correspondingly) according to Equ. S4 as a function of the molar ratio x. QDs are solvated at RT in toluene and ligated with TOPO. Data for I_0/I have been selected only for comparable concentrations to those from $<\tau_0>/<\tau>$ [3, 4].

From this we conclude that both observables follow the same quenching mechanism. Figures S1 and 2C show that the time resolved PL at $x = 8$ reveals mainly very fast components upon assembly formation. Evaluation of previous data [4] shows (with a better time resolution than in the present experiments) considerably smaller $K_{SV}{}^{D}\ (I) \approx K_{SV}{}^{D}\ (\tau_0)$ values. (The reasons of smaller $K^{D}{}_{SV}\ (I(x)) \approx K^{D}{}_{SV}\ (\tau(x))$ values in the latter case may be due to the different type of QD, namely CdSe/ZnS(RQD) [3, 5].

A discrepancy between $K_{SV}{}^{D}(I(x))$ and $K_{SV}{}^{D}(\tau(x))$ might have two reasons: *(i)* The presence

of at least 2 different quenching mechanisms *e. g.* one in the ground state and another one in the excited state or/and *(ii)* experimental time resolution is limited thus missing extremely fast decay processes (faster than 800 fs) which contribute to the PL intensity quenching as "dark" states but are missed in time-resolved experiments. We never observed changes in absorption upon assembly formation which makes reason *(i)* very unlikely to apply.

Figure S3 shows an analysis of the PL decay of CdSe/ZnS(RQD) (top) and the one of (m-Pyr)$_4$H$_2$P (bottom) at x = 4.5 (taken from [5]). The (m-Pyr)$_4$H$_2$P fluorescence shows a build-up component (not observed in the absence of QDs) of about 2-3 ns and an average fluorescence decay of 11 ns for (m-Pyr)$_4$H$_2$P (Figure S3 bottom). The latter is by about 2 - 3 ns longer than the intrinsic (m-Pyr)$_4$H$_2$P decay (Figure S3 middle) under otherwise identical conditions. More qualitative, Figure S3 shows that the distribution of (m-Pyr)$_4$H$_2$P decay times becomes slightly broader upon nanoassemby formation and is on average shifted to longer times (Figure S3 bottom). Moreover, corresponding to the fluorescence build-up times we find PL QD decay times in the same time range (Figure S3 top).

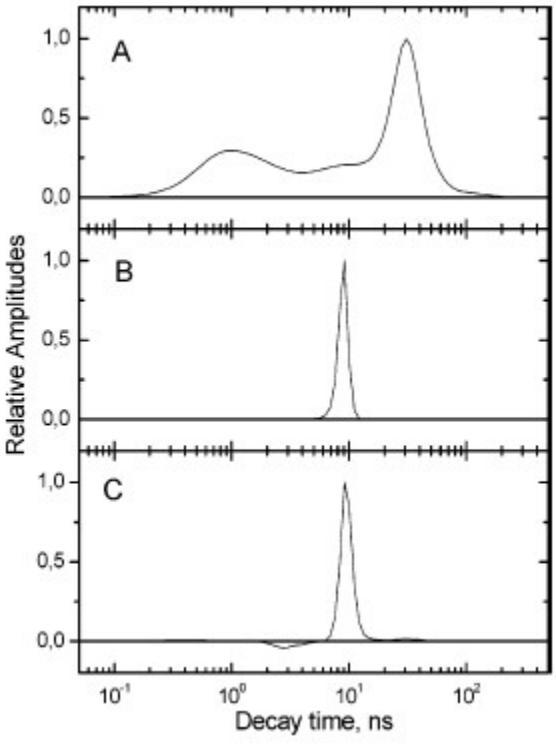

Figure S3 Decay amplitude distributions for CdSe/ZnS(RQD) (top), non-complexed (m-Pyr)$_4$H$_2$P (middle) and (m-Pyr)$_4$H$_2$P at x = 4.5 (bottom) (from [4] with permission).

References

[1] J. R. Lakowicz. Principles of Fluorescence Spectroscopy. *Springer* (2006) New York.

[2] E. Zenkevich, C. von Borczyskowski. Self-Assembled Organic-Inorganic Nanostructures: Optics and Dynamics. E. Zenkevich, C. von Borczyskowski (Eds.) *Pan Stanford* (2016) Singapore.

[3] T. Blaudeck, E. Zenkevich, F. Cichos, C. von Borczyskowski. Probing Wave Functions at

Semiconductor Quantum Dot Surfaces by Non-FRET Photoluminescence Quenching. *J. Phys. Chem. C* (2008) **112** 20251–20257.
[4] E. Zenkevich, F. Cichos, A. Shulga, E. Petrov, T. Blaudeck, C. von Borczyskowski. Nanoassemblies designed from semiconductor quantum dots and molecular arrays. *J. Phys. Chem. B* (2005) **109** 8679-8692.
[5] T. Blaudeck, E. Zenkevich, M. Abdel-Mottaleb, K. Szwaykowska, D. Kowerko, F. Cichos, C. von Borczyskowski. Formation Principles and Ligand Dynamics for Nanoassemblies of CdSe Quantum Dots and Functionalized Dye Molecules. *ChemPhysChem* (2012) **13** 959-972.

S5 Spectral Properties of Intra-Gap Emission (IGE)

Not only CdSe/ZnS(HY) and CdSe(SO) QDs show the existence of long wavelength PL emission (in addition to the NBE PL, see Figure 4 in the manuscript), but weak PL of deep (intra-gap) and shallow traps (or surface states) is also observed for other QDs. Figure S4 shows PL across a wide spectral range for CdSe/ZnS(CG) (A) and CdSe/ZnS(LPB) (B).

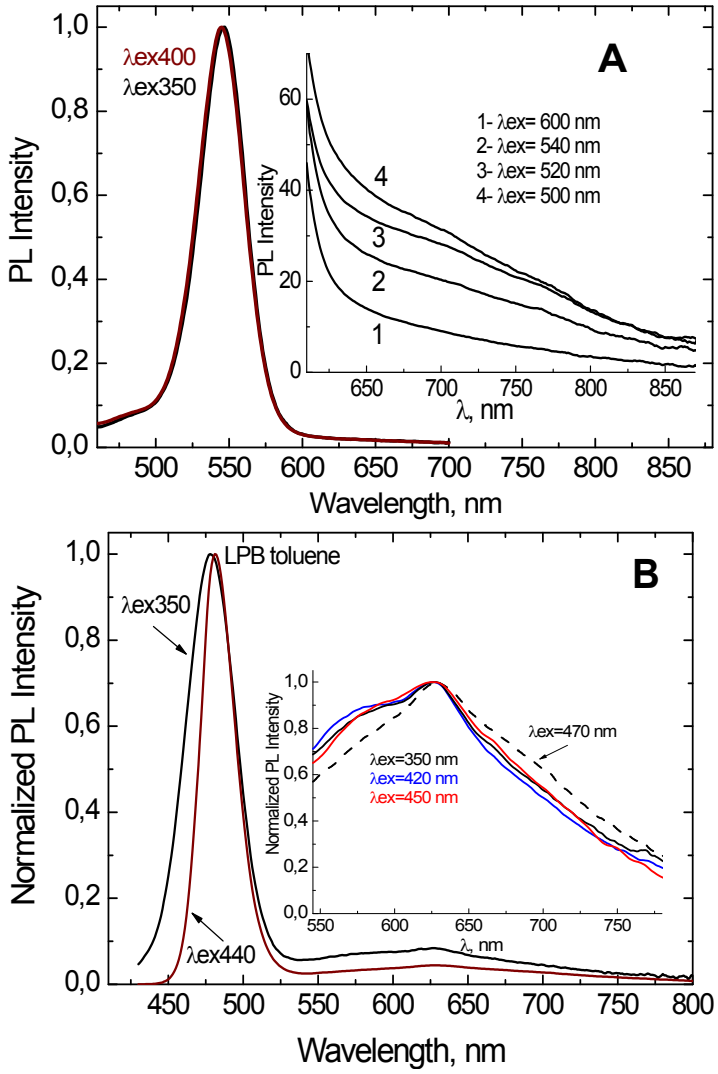

Figure S4. Photoluminescence spectra of (**A**) CdSe/ZnS(CG) and (**B**) CdSe/ZnS(LPB) (toluene, RT, TOPO capped) as a function of excitation wavelengths. The insets show the amplified PL emission across a broad wavelength range. **A**: IGE is very weak at all excitation wavelengths. **B**: Line narrowing upon variation of excitation energy is caused by size selection. Variation of excitation

reveals the presence of 3 distinct bands, a narrow one at 628 nm and 2 broad ones between 550 – 625 nm and 630 – 750 nm, respectively. The latter one is more effectively excited with NBE excitation. The narrow band was not observed in earlier spectra (see Figure 4) and is probably due to formation of lager CdSe/ZnS(LPB) QDs upon long time investigations.

The question arises whether IGE can be excited directly at energies below excitonic absorption. Figure S5 shows via absorption and PLE data that at least part of the IGE can be excited directly.

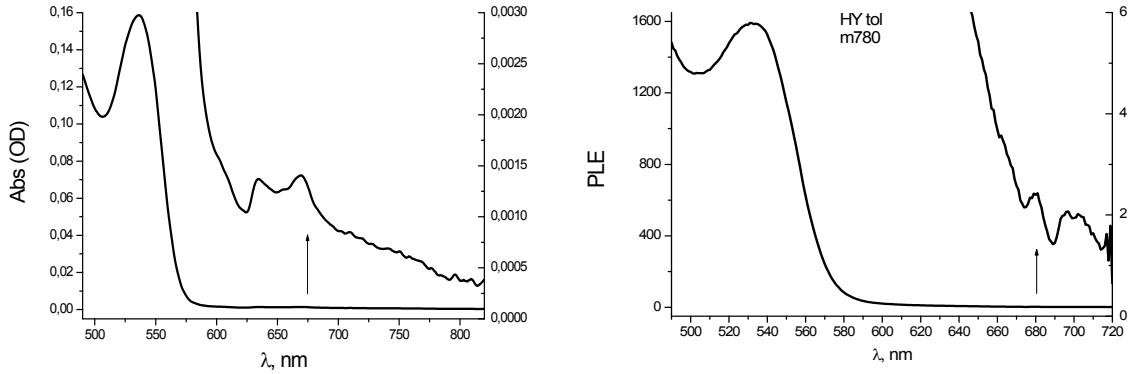

Figure S5 Left: Absorption spectrum of CdSe/ZnS(HY) in toluene at ambient temperature. The shoulder at 580 – 625 nm is assigned to shallow trap states (see Figures 5B and 5C in the manuscript). **Right:** PLE with detection wavelength at 780 nm. PLE sets in at about 670 nm. We were not able to detect PLE for wavelength > 720 nm but observed weak absorption up to about 770 nm. Since the PL intensity of IGE is extremely weak it is difficult to decide whether structures indicated by an arrow are real though PLE excitation spectra have been corrected for spurious Raman lines.

In Figure S5 we show both for absorption and PLE that IG states can be excited directly though at very low probability. After normalization of emission intensities for both spectra we arrive at the conclusion that IGE < 720 nm shows upon direct IG excitation relatively enhanced emission intensity in PLE as compared to absorption in this range. This indicates that shallow traps (ST) are involved in population of corresponding IG states < 720 nm. Emission > 720 nm is compared to PLE more effectively generated by direct absorption into IG states far below NBE.

A comparison of normalized PLE and absorption (ABS) in Figure S6 shows for CdSe(SO) that IGE is more effectively excited at excitation energies above the first exciton band which indicates the involvement of hot electrons upon generation of IGE.

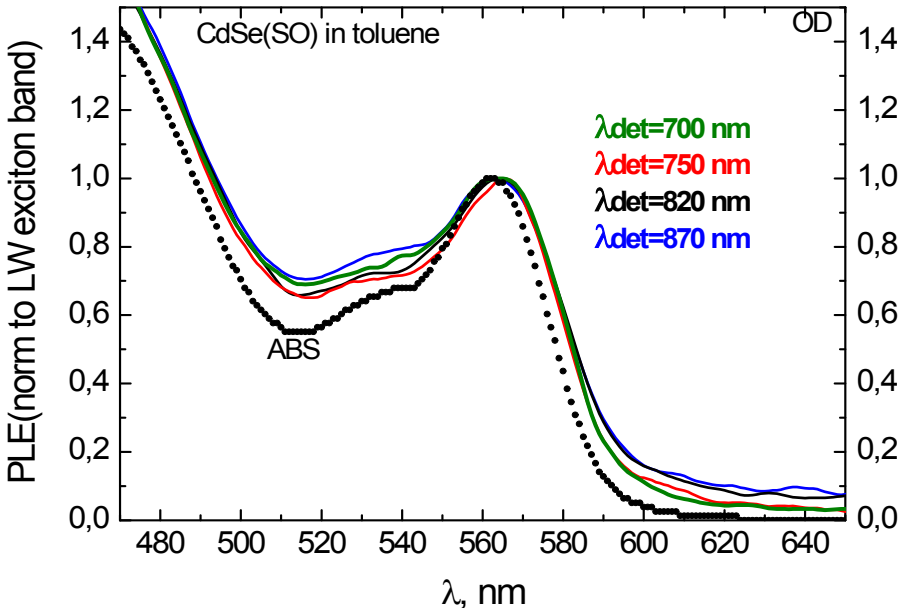

Figure S6 PLE spectra at various detection wavelengths in the range of intra-gap emission (IGE) of TOPO capped CdSe(SO) in toluene at ambient temperature. The dotted line represents the absorption in form of the optical density (OD). Comparison shows that IGE is with respect to OD more effectively excited below the typical NBE and for excitation at high exciton energies (hot electrons). PLE at 820 and 870 nm reveals that excitation below NBE is relatively more effective than for PLE ≤ 750 nm.

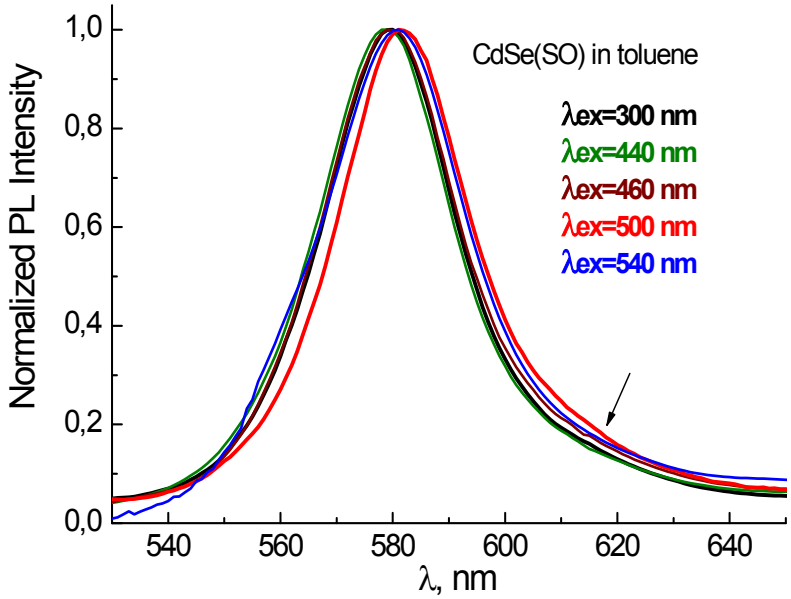

Figure S7 NBE PL spectra of TOPO capped CdSe(SO) QD in toluene at various excitation wavelengths in the NBE range at ambient temperature. The arrow shows a shoulder at 620 nm which probably belongs to shallow trap emission. Excitation wavelengths of 500 and 540 nm show the influence of size selection.

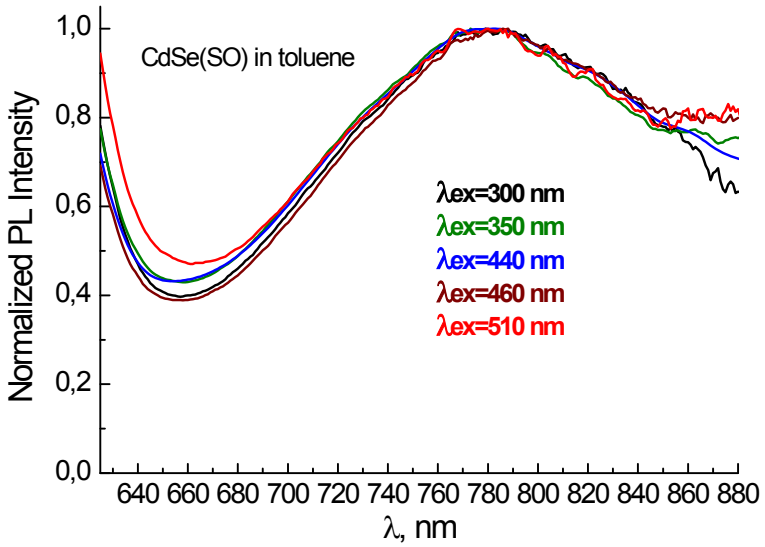

Figure S8 Long wavelength emission for CdSe(SO) in toluene at ambient temperature at various exitation wavelengths. IGE spectra are nearly identical for excitation into energetically highly excited exciton states.

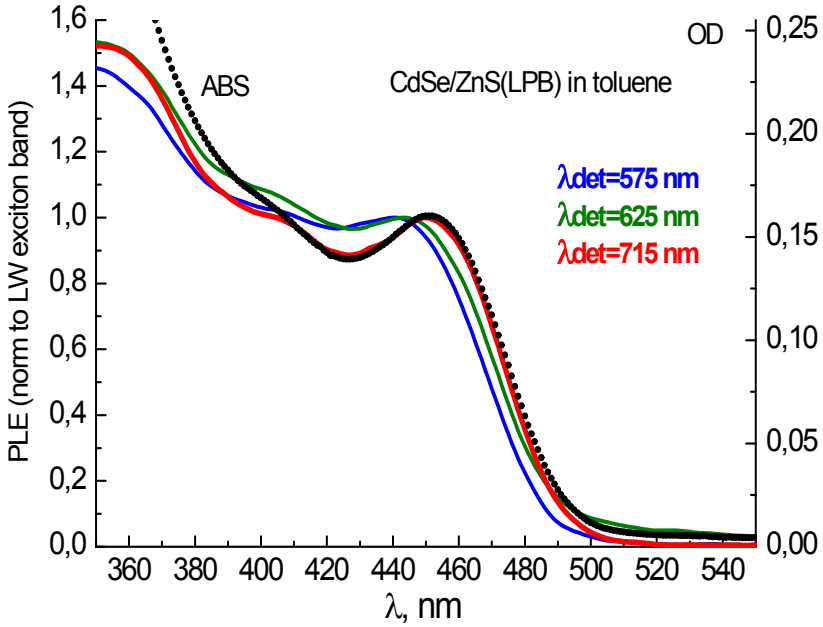

Figure S9 PLE spectra at detection wavelengths (625 and 715 nm) in the range of IGE and NBE PL (575 nm) of TOPO capped CdSe/ZnS(LPB) in toluene at ambient temperature. The dotted line represents the absorption (ABS) in form of the optical density (OD). (See for comparison PL spectra in Figure 5.

Interestingly, CdSe/ZnS(LPB) IGE has 3 bands (2 broad, 1 narrow (628 nm), all show CdSe/ZnS(LPB) PLE spectra. With respect to broad IGE the energetically lowest band is more effectively excited at NBE excitation as compared to detection at 575 nm. This

observation is in line with IGE of CdSe/ZnS(HY) as a function of excitation energy (see Figure 5A in the main text). However, it is different with respect to PLE spectra of CdSe(SO) (see Figure S6). Possibly, shallow traps are less abundant in capped CdSe/ZnS QDs as compared to uncapped CdSe(SO), which is already obvious comparing the respective PL in Figure 4. This interpretation is supported by inspecting PLE of CdSe/ZnS(CG) in Figure S10. Additionally, excitation of very hot excitons does not as effectively result in IGE for CdSe/ZnS(LPB) as compared to CdSe(SO).

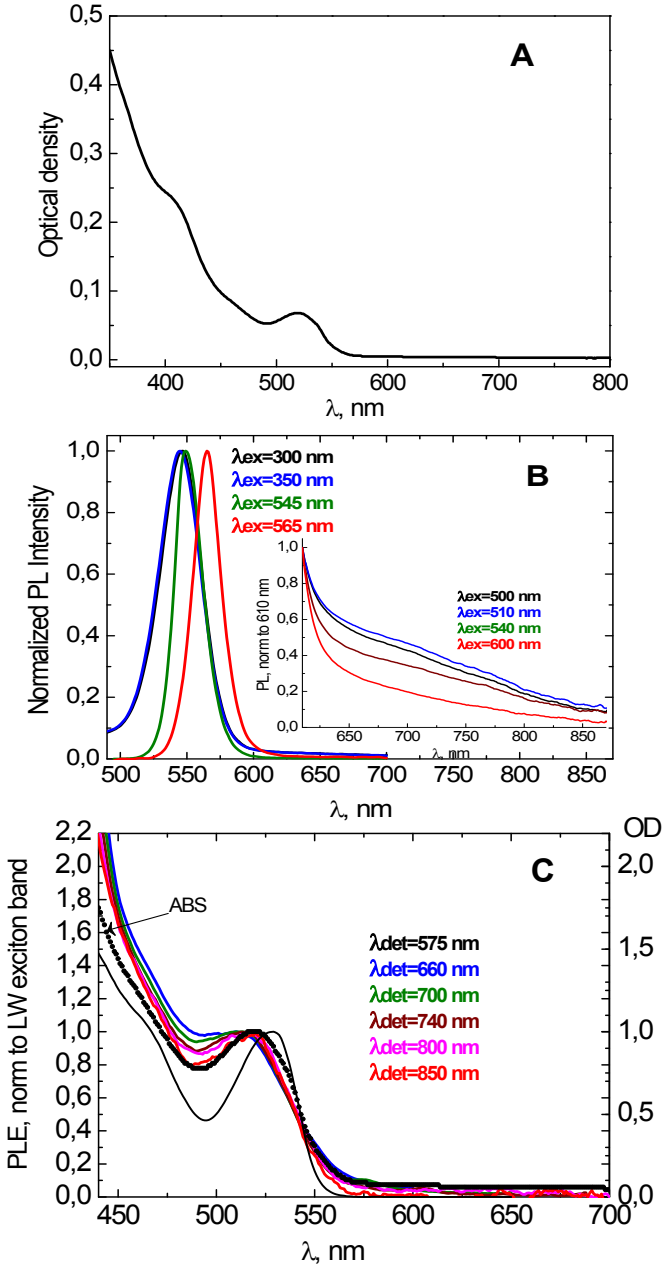

Figure S10 Absorption (**A**), photoluminescence (**B**) and PLE (**C**) spectra for TOPO capped CdSe/ZnS(CG) QDs in toluene at ambient temperature at various excitation (**B**) and detection (**C**) wavelengths in a wide spectral range. The inset in (**B**) shows the PL emission in the long wavelength range. CdSe/ZnS(CG) shows a very similar behaviour as CdSe/ZnS(LPB) besides the fact that IGE

generation is very effective also at high excitation energies. It is obvious that NBE PL is in comparison with absorption less effectively generated than IGE. Again, IGE at wavelengths > 550 nm can be generated via absorption but not so effective via shallow trap (ST) excitation (see also Figure S5).

S6 Wavelength Dependent PL Dynamics of QDs

PL of all investigated QDs consists - depending on the specific type - out of near-band edge (NBE) PL, shallow trap (ST) emission and intra-gap emission (IGE). IGE is energetically very broad and its relative intensity with respect to NBE PL depends critically on the crystal quality and is according to our findings especially strong for uncapped and very small QDs. PL decay times vary across the total emission wavelength.

The multi-exponentiality of the CdSe/ZnS(HY) PL decay is qualitatively similar to the one of CdSe(SO). We show in Figure S11 the PL decay detected at 555 nm (NBE) and 700 nm (intensity maximum of IGE). It is evident that the longest decay time at 700 nm detection is much longer than to be unraveled at the laser limited time of 450 ns repetition time. Though the overall decay time scale is much longer at 700 nm as compared to 555 nm detection a short decay time of a few ns is visible also for 700 nm detection.

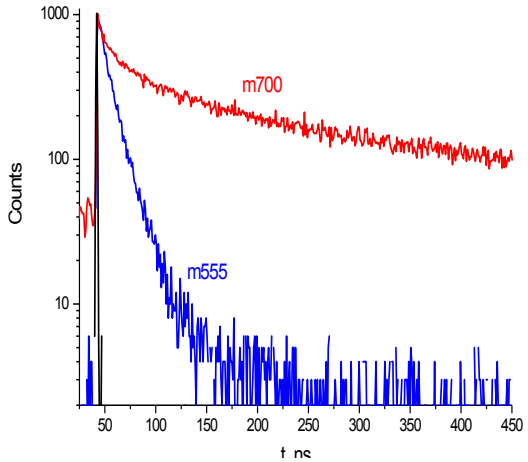

Figure S11 PL decay of TOPO capped CdSe/ZnS(HY) in toluene at RT at detection wavelengths of 555 nm and 700 nm, respectively. The instrumental response function is also shown in black. Excitation is at 440 nm. Absolute intensities of the 2 bands differ almost by 2 orders of magnitude.

As we have discussed in the contribution the presence of build-up dynamics is of special interest both for QD PL and H_2P fluorescence. Firstly, we investigated whether QDs show such dynamics also in the absence of nanoassembly formation. The build-up time of QD PL is in all investigated cases at the limit of our time resolution and faster than 1 ns. We show in Figure S12 the build-up dynamics for CdSe/ZnS(HY) at 2 different detection wavelengths, namely in the range of the NBL PL at 550 nm and in the range of IG states at 630 nm. The

build-up time is within the experimental response at 550 nm while it is slightly slowed down to about 1 ns at 630 nm. The same applies at 700 nm (see Figure S12). This can be explained by assuming that intra-gap states are at least partly populated via short lived near band edge states.

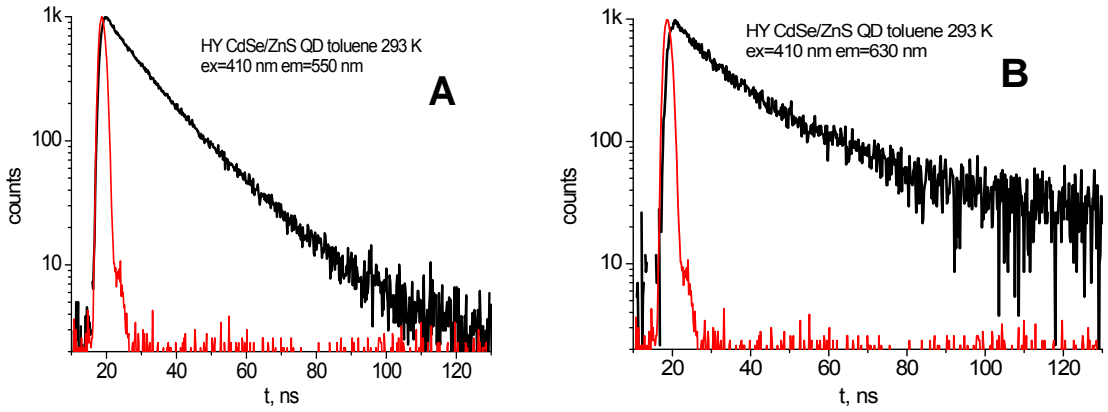

Figure S12 PL decay of CdSe/ZnS(HY) in toluene at RT and 410 nm excitation wavelength. Also shown is the experimental response function in red. **A:** Near-band-edge emission at 550 nm. **B:** Intra-gap emission at 630 nm.

Figure S13 shows PL decays of CdSe/ZnS(CG) detected at 545 nm (NBE) and 700 nm (intensity maximum of IGE). It is clearly seen that the longest decay time at 700 nm detection is much longer with respect to NBE emission. Again, the build-up time is slightly longer at 700 nm.

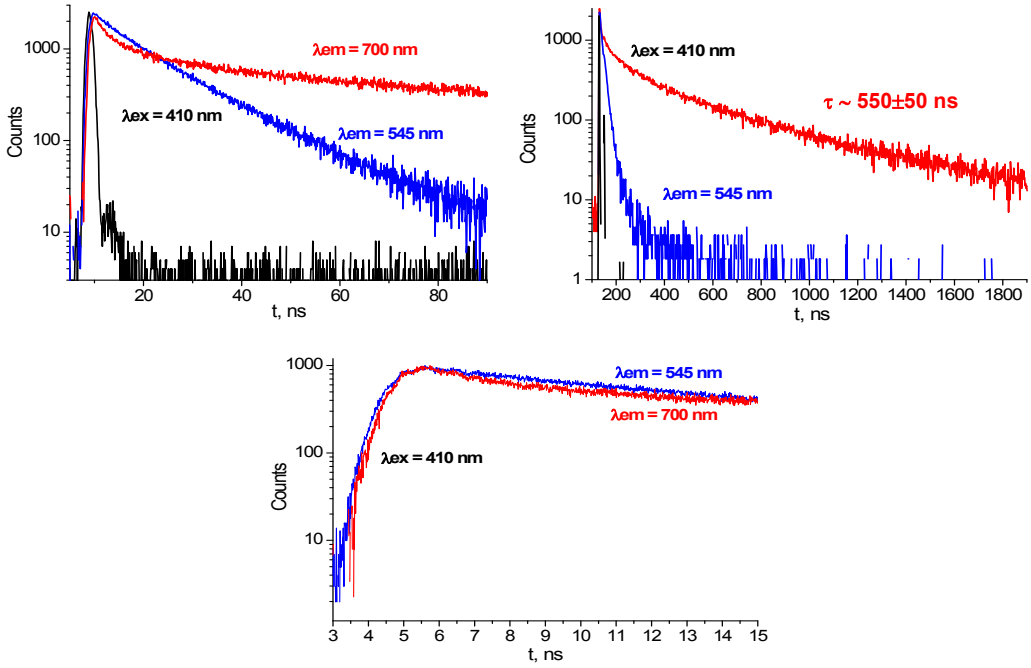

Figure S13 Intensity normalized PL decays of TOPO capped CdSe/ZnS(CG) detected at 545 nm (NBE) and 700 nm (maximum of IGE) detected at 3different time resolutions in toluene at RT. The experimental response function is also shown.

Finally, the analysis of experimental PL decays for a QD without ZnS shell, CdSe(SO), (Figure S14) confirms the above conclusions.

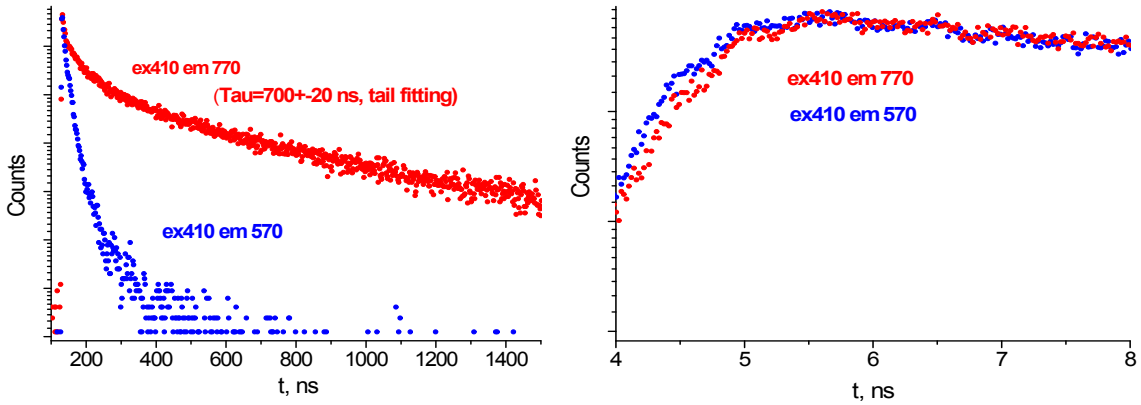

Figure S14 PL decays of TOPO capped CdSe(SO) detected at 570 nm (NBE) and 770 nm (intensity maximum of IGE) detected at different time resolution in toluene at RT.

Figure S15 shows qualitatively the distribution of dynamic ranges across an inhomogeneously broadened spectral PL band of a QD. It includes the influence of imperfect crystal growing processes (see also Chapter S9).

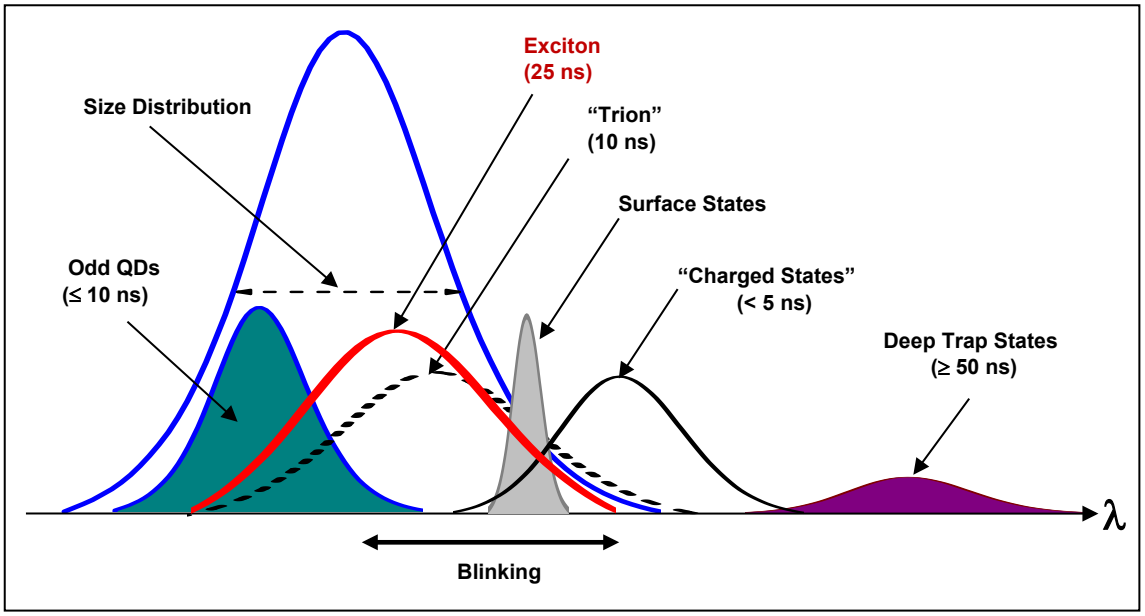

Figure S15 Schematic presentation of QD PL band(s) caused by various reasons. Typical decay times are indicated. Size distributed QDs establish at least 2 classes, namely excitons and (small) QDs with many surface defects "Odd QDs" and increased non-radiative PL decay. Relative intensities (and widths) have been arbitrarily chosen. Blinking is occurring among excitons, "trions", and "charged states". PL build-up times are for all states faster than 1 ns and are preferentially excited via hot exciton bands or direct excitation.

Figure S15 shows the overall PL linewidth caused by the size distribution. The inhomogeneous spectral line is further broadened by the energetic distribution of various electronic states which are

partly interrelated by PL intensity blinking with synchronous spectral shifts and life time fluctuations. The electronic states are related to excitons, trions, shallow and deep traps. Charged states are also included. These short lived states are subject to red-shifting Stark effects [1, 2]. Additionally, on the high energy side imperfect QDs with many surface states show up which are caused by imperfect growing processes. These states are short lived [3].

References

[1] R. Schmidt, C. Krasselt, C. Göhler, C. von Borczyskowski. The Fluorescence Intermittency for Quantum Dot Is Not Power-Law Distributed: A Luminescence Intensity Resolved Approach. *ACS Nano* (2014) **8** 3506-3521.

[2] I. Trenkmann, C. Göhler, C. Krasselt, C. von Borczyskowski. Tuning Luminescence Intermittency, in: Tuning Semiconducting and Metallic Quantum Dots: Spectroscopy and Dynamics, p. 283-376, C. von Borczyskowski, E. Zenkevich (Eds.) *Pan Stanford Publishers* (2016) Singapore.

[3] A. L. Rogach, T. Franzl, T. A. Klar, J. Feldmann, N. Gaponik, V. Lesnyak, A. Shavel, A. Eychmueller, Y. P. Rakovich, J. F. Donegan. Aqueous Synthesis of Thiol-Capped CdTe Nanocrystals: State-of-the-Art *J. Phys. Chem. C* (2007) **111** 14628-14637.

S7 FRET related Foerster Parameters

The evaluation of experimental FRET efficiencies in QD/porphyrin nanoassemblies on the base of the measured porphyrin fluorescence intensity has been described in Section S2. Here, we give a short summary how to evaluate theoretically Foerster parameters for the systems under consideration (described in details by us earlier [1, 2].

It was shown earlier [2] and references therein that QD/Dye nanoassemblies are best described in the weak coupling regime which allows the application of the Foerster model for fluorescence resonant energy transfer (FRET). In addition, we have shown for QD/Porphyrin nanoassemblies [2, 3] that QD PL quenching efficiency does not depend on redox properties of porphyrin molecules since the porphyrin fluorescence is not quenched. This implies that typical photoinduced charge transfer processes do not play the dominant role in the observed QD PL quenching in the systems under study.

Correspondingly, if other QD PL quenching channels in QD/Dye nanoassemblies are absent we expect that FRET from a photoexcited QD (donor (D)) to a lower-energy dye molecule (acceptor (A)) takes place due to the coupling of the emission dipole moment of the QD exciton of *D* with the absorption dipole moment of the nearby *A* chromophores. This allows the application of Foerster model for FRET which is typically used in the limit of "localized oscillators" as a result of the electric dipole approximation. Notably, on the base of experimental data for CdSe/ZnS QDs and dye molecules (porphyrins or perylene diimides) the effective transition dipole length $|l|$ is $|l| \leq$ 1-2.0 Å for dyes and $|l| \approx$ 2.0 Å for QDs under study [1], while estimations of inter-centre D-A distances R_{DA} for the optimized structures of

QD/Dye nanoassemblies give values $R_{DA} \approx 26 \div 36.6$ Å [1, 2, 3, 4, 5]. Since $|l| << R_{DA}$ the point dipole-dipole approximation is still valid or QD/Dye nanoassemblies.

Consequently, FRET rate constant k_{FRET} for an isolated *D-A* pair at distance R_{DA} is calculated according to [6, 7]

$$k_{FRET} = \frac{1}{\tau_D^0} \cdot \frac{R_0^6}{R_{DA}^6} \quad , \tag{S5}$$

where τ_D^0 is the emission decay time of the individual donor in absence of the acceptor and R_{DA} is the inter-center distance of the interacting dipoles. R_0 is the critical Foerster radius which may be calculated as

$$\left(R_0^{\text{theor}}\right)^6 = \frac{9000 \ln 10 k^2 \varphi_D^0}{128 \pi^5 n^4 N_A} \times \int_0^\infty f_D(\nu) \varepsilon_A(\nu) \frac{d\nu}{\nu^4} . \tag{S6}$$

where $N_A = 6.022 \cdot 10^{23}$ M^{-1} is Avogadro number, φ_D^0 the emission quantum efficiency in the absence of FRET and n the refraction index of the solvent. The orientation factor is $k^2 = [\cos(\mu_D, \mu_A) - 3 \cos(\mu_D, r_{DA}) \cdot \cos(\mu_A, r_{DA})]^2$, where (μ_D, μ_A) is the angle between transition dipole moment vectors of the D and A subunits. (μ_D, r_{DA}) and (μ_A, r_{DA}) denote the angles between the dipole vectors of D and A and the direction D→A, respectively. For a random static distribution of interacting dipoles k^2 becomes 0.476 [7]. This is the case for QD-Dye nanoassemblies. The spectral overlap integral

$$J(\nu) = \int_0^\infty f_D(\nu) \varepsilon_A(\nu) \frac{d\nu}{\nu^4} \tag{S7}$$

is calculated on the basis of experimental acceptor molecular absorption and donor (QD) PL spectra, where $\varepsilon(\nu)$ corresponds to the molar decimal extinction coefficient of A, $f_D(\nu)$ to the D quantum emission spectrum normalized to unity by area on a wave number scale. The detailed analysis of theoretical dependencies of spectral overlap, Foerster critical radius R_0, donor-acceptor distance R_{DA}, FRET efficiencies, and reciprocal FRET rate as a function of the QD size represented by the respective PL emission wavelength and one type of porphyrin (m-Pyr)$_4$H$_2$P molecule has been described by us recently [2].

Furthermore, if FRET plays the dominant role in QD PL quenching in nanoassemblies, the theoretical FRET efficiency Φ_{FRET}^{theor} for (1:1) pair interaction QD-Dye can be calculated as

$$\Phi_{\text{FRET}}^{\text{theor}} = \left[1 + \left(R_{DA} \Big/ R_0^{\text{theor}}\right)^6\right]^{-1} . \tag{S8}$$

When a finite number of acceptors become attached to the QD surface, the excitonic energy is spread among n acceptors on one QD with equal probability. Generally speaking, the

probability of an exciton transfer to particular acceptor molecules scales inversely proportional to the total number of n acceptors A per donor D. Thus, Eq. S8 becomes [8]

$$\Phi_{FRET}^{theor}(n) = \left[1 + \frac{1}{n}\left(R_{DA} \Big/ R_0^{theor}\right)^6\right]^{-1}. \qquad (S9)$$

Based on these physical backgrounds the comparative theoretical analysis of FRET parameters for various QD/Dye nanoassemblies has been carried out in our group [1, 5, 9]. These calculations yield that if FRET is the only reason of QD PL quenching in nanoassemblies, already upon attachment of one single acceptor molecule, the maximal achievable FRET efficiency may reach up to 50-70% for various CdSe/ZnS QDs (depending on the QD PL quantum yield). Additionally, theoretical estimations show that for the nanoassembly containing CdSe/ZnS QD ($d_{CdSe} \geq 3$ nm, 2 ZnS monolayers) or CdSe(SO) QD ($d_{CdSe} = 3.5$ nm) with attached meta-pyridyl substituted porphyrin, FRET should be realized within a time scale longer than 10 ns (even up to 30÷37 ns for CdSe/ZnS(RQD), see Table 1 in [1]).

In addition, it should be mentioned that FRET dynamics between a CdSe/ZnS QD and a porphyrin molecule in a QD/porphyrin nanoassembly have also been studied by *ab initio* electronic structure calculations (reduced density matrix formalism) combined with a molecular dynamic approach [4]. According to this approach in the case of even smaller $Cd_{33}Se_{33}/Zn_{78}S_{78}$ QDs with an attached porphyrin molecule, FRET QD→Porphyrin should occur on a nanosecond time scale shorter than 7 ns.

As a consequence, if one does not take into account a competition with other reasons for QD PL quenching, the real transfer time based on atomistic details derived from PL quenching in QD/Porphyrin nanoassemblies may be fully described in the framework of the Foerster model. Theoretically predicted FRET times should range from ~7 ns to 37 ns.

We like to discuss at this point previously reported FRET dynamics for CdSe/ZnS(RQD) QDs which should have much less effective FRET compared to CdSe(SO) [1, 2]. Previously we have shown [10] that if a FRET donor decay time is longer than the one of the acceptor there will be still energy transfer lasting longer than the acceptors intrinsic decay time resulting in an apparent lengthening of the fluorescence decay which is in fact observed for CdSe/ZnS(RQD) as is shown in Figure S3 (and CdSe(SO), see manuscript). In such case we expect for CdSe/ZnS(RQD) nanoassemblies a bi-exponential decay of the acceptor fluorescence with k_{H2P} and an additional "effective" energy transfer rate according to (k_{FRET} + k_{QD}). Taking the PL decay of the CdSe/ZnS (RQD) based nanoassemblies of 20 ns and the FRET transfer time of 30 ns [1] we obtain 12 ns for the second component of the postulated

bi-exponential H_2P decay which is qualitatively in agreement with a broadening of the fluorescence decay time of H_2P (see Figure S3).

The observed short build-up component of 3 ns is much too fast to be responsible for FRET QD→porphyrin for this kind of QD (d_{CdSe} = 3.2 nm, 3 ZnS monolayers). Therefore, we assign this component also for CdSe/ZnS(RQD) to the population time of those intra-gap trap states induced by H_2P or effectively populated in the presence of H_2P molecules on a QD surface.

Table 1 contains for CdS/ZnS(HY)-H_2P experimental PL decay times in comparison to calculated ones. For details see manuscript.

Table S1 Experimental τ_i and according to Equ. 5 (see manuscript) calculated PL decay times $\tau_{i(calc)}$, relative normalized amplitudes A_i and intensities $I_i = (A_i \cdot \tau_i)$ for CdSe/ZnS(HY) and their related assemblies with H_2P in toluene at ambient temperature.

Parameter[1)]	CdSe/ZnS(HY)[2)]	CdSe/ZnS (HY)-H_2P[3), 4)]
τ_1	1	0.45
A_1	0.35	0.69
I_1	0.35	0.31
τ_2	7	4.5
A_2	0.36	0.17
I_2	2.52	0.77
τ_3	18	17
A_3	0.29	0.14
I_3	5.22	2.38

[1)] τ_i in ns; [2)] /1/; [3)] PL decay times taking FRET according the Foerster model with n = 1 into account (See Equ. 5 in manuscript). Amplitudes A_i are taken from experiment. [4)] Quantum Yield 0.41 /1/.

An additional reason of QD PL quenching in QD-H_2P nanoassemblies may be caused by photoinduced electron transfer (PET) from CdSe QDs to attached porphyrin molecules. The possibility of PET specific processes in QD-porphyrin nanoassemblies has been discussed in few papers [11, 12] upon theoretical analysis of experimental data on PL features and quenching mechanisms of water-soluble CdSe/ZnS QDs (d_{CdSe} = 2.8 nm) by attached cationic porphyrins ($H_2TMPyrP^{4+}$ and $ZnTMPyrP^{4+}$) in solution with high polarity (water at pH 5.5). In these QD-porphyrin nanoassemblies, long-range inductive resonance electronic excitation energy transfer takes place from surface modified (with thioglycolic or mercaptoundecanoic acid) QDs to porphyrin ligands, which leads to QD PL quenching and an increase of the

porphyrin fluorescence intensity. It has been shown that, when mercaptoundecanoic acid is used as a QD shell, the QD luminescence quenching efficiency by porphyrins follows the Förster-Galanin theory and depends on the overlap integral between the CdSe/ZnS luminescence band and the absorption spectra of free-base porphyrin $H_2TMPyrP^{4+}$ and its metal complex $ZnTMPyrP^{4+}$. It has been found that upon decrease of QDs ↔ Zn-porphyrin intercenter distance from 39.1 (mercaptoundecanoic acid) to 30.1, a considerable QD PL quenching is observed. However, FRET efficiency substantially decreases, from 55% in the former case to 23% in the latter one. Based on quantum-chemical calculations (density function theory and polarisable continuum model) it has been concluded that in polar solvents the PL low quantum yield for CdSe/ZnS QDs passivated by residues of mercaptocarboxylic acids $S^{-}(CH_2)_n COO^{-}$ and its dependence on the number of CH_2 groups are related to the possibility of photoinduced electron transfer from the HOMO of passivating molecules to QDs (QD* ⇐ $S^{-}(CH_2)nCOO^{-}$ hole transfer). It has been shown that QD PL quenching in nanoassemblies CdSe/ZnS(thioglycolic acid) - $ZnTMPyrP^{4+}$, which is complementary to the energy transfer, may be caused also by the photoinduced electron transfer that involves the participation of the LUMO of the $ZnTMPyrP^{4+}$ molecule (QD* ⇒ $ZnTMPyrP^{4+}$). So, for QD-porphyrin nanoassemblies in non-polar solvents, the realization of effective photoinduced charge transfer processes with participation of excited states of porphyrin ligand seems to be low probable.

References

[1] E. Zenkevich, F. Cichos, A. Shulga, E. Petrov, T. Blaudeck, C. von Borczyskowski. Nanoassemblies designed from semiconductor quantum dots and molecular arrays. *J. Phys. Chem. B* (2005) **109** 8679-8692.

[2] E. Zenkevich, C. von Borczyskowski. Structural and Energetic Dynamics in Quantum Dot- Dye Nanoassemblies, in: *Self-Assembled Organic-Inorganic Nanostructures: Optics and Dynamics*, p. 1-147. E. Zenkevich, C. von Borczyskowski (Eds.), Pan Stanford Publishers (2016) Singapore.

[3] T. Blaudeck. Self-Assembly of Functionalized Porphyrin Molecules on Semiconductor Nanocrystal Surfaces. *PhD Thesis* (2007) TU Chemnitz.

[4] D. S. Kilin, K. Tsemekhman, O. V. Prezhdo, E. I. Zenkevich, C. von Borczyskowski. Ab Initio Study of Transfer Dynamics from a Core-Shell Semiconductor Quantum Dot to a Porphyrin Sensitizer. *J. Photochem. Photobiol. A* (2007) **190** 342-351.

[5] D. Kowerko, J. Schuster, N. Amecke, M. Abdel-Mottaleb, R. Dobrawa, F. Würthner, C. von Borczyskowski. FRET and ligand related NON-FRET processes in single quantum dot-perylene bisimide assemblies. *PhysChemChemPhys* (2010) **12** 4112-4123.

[6] Foerster, T. Modern Quantum Chemistry. O. Sinanoglu (Ed.) *Academic Press* (1965) New York)

[7] V. M. Agranovich, M. D. Galanin. Electronic Excitation Energy Transfer in Condensed Matter. *North-Holland Pub. Co*. (1982) Amsterdam, New York.

[8] A. Clapp, I. Medintz, J. Mauro, B. Fisher, M. Bawendi, H. Mattoussi. Fluorescence resonance energy transfer between quantum dot donors and dye-labeled protein acceptors. *J. Am. Chem. Soc.* (2004) **126** 301-310.

[9] C. von Borczyskowski, E. Zenkevich. Formation Principles and Exciton Relaxation in Semiconductor Quantum Dot-Dye Nanoassemblies, in: *Quantum Dot Molecules, Lecture Notes in Nanoscale Science and Technology*, p. 77-148. J. Wu, Z. M. Wang (Eds.) *Springer* (2014) New

York, Heidelberg, Dordrecht, London.
[10] U. Rempel, S. Meyer, B. von Maltzan, C. von Borczyskowski. Energy transfer and distance independent charge separation in self-organised porphyrin-quinone aggregates. *J. Luminesc.* (1989) **78** 97-110.
[11] N.V. Ivashin, E.E. Shchupak, E.I. Sagun. Photoinduced energy and electron transfer processes in self-assembling complexes of CdSe/ZnS water-soluble nanocrystals and cationic porphyrins. *In Proceedings of the International Conference "Nanomeeting-2013". Physics, Chemistry and Applications of Nanostructures. Reviews and Short Notes* (May 28-31, 2013; V.E. Borisenko, S. V. Gaponenko, V. S. Gurin, C.H. Kam, Eds.), World Scientific Publishing Co., New Jersey, London, Singapore, Bejing, Shanghai, Hong-Kong, Taipei, Chennai. (2013) p. 573-576.
[12] E.I. Sagun, V.N. Knyukshto, N.V. Ivashin, E.E. Shchupak, G.K. Zhavnerko, N.V. Karatai, V.E. Agabekov. Photoinduced relaxation processes in self-assembling complexes based on water-soluble CdSe/ZnS nanocrystals and cationic porphyrins. *Optics and Spectroscopy* (2012) **113**, 165-178.

S8 Nanoassembly Formation

It is known [1-3] than in liquid non-polar solutions only about 30% of the dangling (Zn) bonds of the investigated CdSe/ZnS QDs (with d_{CdSe}=2.5÷3.0 nm and 2 ZnS monolayers of *l*=1 nm) are "saturated" by TOPO ligands due to ligand-related steric constraints. This conclusion is confirmed also by X-ray data [4]. Porphyrin-type ligands [5,6] as well other organic molecules with appropriate functionalized side anchoring groups [7-11] are expected to bind to QD surface sites by substitution of the surfactant ligands (TOPO or long-chain amines or thiols) present from the synthesis stage. As we have shown earlier [5] the formation of nanoassemblies based on TOPO-capped CdSe/ZnS QDs and (*5, 10, 15, 20*)-meta-pyridyl-porphyrin molecules is realized via two-point interaction of two *meta*-nitrogens of two *meso*-phenyl rings with two Zn atoms of QD surface (see Scheme 1 in the manuscript text).

Based on titration experiments and using pyridyl-substituted porphyrins with various number of pyridyls and different positions of nitrogens (*ortho*-, *meta*- and *para*-) we have argued [5] that because of steric reasons, relatively large volume of porphyrin molecule and small anchoring *meso*-pyridyl substituents as well as ligand exchange competition (TOPO↔porphyrin) on the QD surface, H_2P(*m*-Pyr)$_4$ and H_2P(*p*-Pyr)$_4$ molecules are displaced almost perpendicular on QD surface, while H_2P(*o*-Pyr)$_4$ or H_2P(*o*-Pyr)$_4$ do not practically interact with QD surface. This conclusion has been proven also [12] using molecular mechanics calculations within the HyperChem software package for the geometry optimization (with VASP) for CdSe/ZnS QD-H_2P(*m*-Pyr)$_4$ nanoassembly.

It should be mentioned that the arrangement of porphyrin molecules on QD surface in nanoassemblies may be dependent on few reasons: *(i)* the nature (and size) of passivating surfactant ligands; *(ii)* number of functionalized side anchoring groups (tether chains); *(iii)* length and flexibility of these tether chains. For instance, recently it was shown (based on a combination of ^{1}H NMR, absorption, and fluorescence spectroscopies) [11] that porphyrin

molecules carrying one carboxylate function can interact with monodisperse CdSe QDs with d_{CdSe}=2.2-2,3 nm (coated exclusively with relatively small oleate ligands) to form "porphyrin - CdSe QD" nanoassemblies with porphyrins stacked upright on the CdSe QD surface. On the other hand, it was found in this study [11] that porphyrins having few (3 and 4) long anchoring alkyl-type tether chains (the so-called polydentate porphyrin ligands) are able to bind to QD surface more strongly than monodentate porphyrin. Such polydentate porphyrin ligands attach themselves to QD flat-on, i.e., parallel to the crystal surface. In addition, it was observed that the formation of QD-porphyrin-QD structures (containing one porphyrin ligand being attached to 2 QDs) as well as a larger polymeric nanoassemblies $[QD\text{-}porphyrin\text{-}QD]_n$ is followed by precipitation process and loss of colloidal stability.

Precipitation effects were not observed in our experiments. The low probability for the formation QD-porphyrin-QD or polymeric $[QD\text{-}porphyrin\text{-}QD]_n$ nanoassemblies in our case seems to be due to few reasons: (*i*) because of a large hydrodynamic volume of QDs the diffusion of QDs is restricted essentially, and at low concentration ($C<10^{-5}$ M) the near displacement of two QDs may not be efficiently realized; (*ii*) steric hindrances between to one QD attached tetra-pyridyl porphyrin molecule and TOPO molecules belonging to the other QD should prevent and effective ligand exchange leading to the attachments of the second QD to QD-H_2P nanoassembly. Additionally, one has to consider the following: (*i*) at molar ratio x = 1 not all constituents might form assemblies, even less than expected according to a Poisson distribution; (*ii*) As has been discussed [13], there might be an upper limit of dye molecules per QD which might be taken into account according to recent publications [13-15].

Finally, it should be mentioned that according to our earlier results [5] the normalization of CdSe/ZnS QD PL quenching to the number of *meso*-pyridyl substituents for various porphyrins showed still more quenching (by roughly a factor of 2 above molar ratio $x = C_{Porphyrin}/C_{QD}$ =2) for 4-pyridyl as compared to 2-pyridyl. It follows from the above discussion that this difference in QD PL quenching might not be considered as indication for binding of 2 QDs to one porphyrin molecule. According to [7, 11], for a given QD concentration and molar ratio x, due to the chelate effect polydentate ligands should bind to the QD surface significantly more strongly than monodentate ligands. Correspondingly, from thermodynamic point of view, the attachment of tetra-pyridyl substituted porphyrin with QD surface is more effective with respect to that for di-pyridyl substituted porphyrin molecule. Namely this difference may be considered as the main reason of the different quenching effect observed

for QD PL upon self-assembly at the same conditions with porphyrin ligands having 2 and 4 *meso*-pyridyl anchoring substituents.

As has been shown in Section S2 FRET efficiencies depend in principle on Poisson statistics of assembly formation [5, 16-19] since a single QD might be statistically assembled with several dye molecules. We identify assembly formation not only via QD PL quenching and FRET enhancement dynamics but also by spectral changes observed for the H_2P acceptor dynamics. It is known that H_2P fluorescence is in first order electric dipole forbidden due to symmetry reasons which results in a relatively long fluorescence decay time (≈ 8 ns) and a relative decrease of the intensity of the Q(0,0) electronic transition compared to that for the vibronic Q(0,1) band [5, 20]. The fluorescence becomes partly allowed by an out-of-plane distortion of the molecule [5].

We explain the lengthening of the H_2P decay upon assembly formation as being due to intercalation of the acceptor into the TOPO ligand shell of the QD which forces H_2P to a more strictly planar conformation. Additional confirmation of our conjecture is provided by recent observations that the assembly formation is accompanied by spectral shifts and changes in the Franck-Condon overlap [5]. We found that H_2P fluorescence in QD-dye nanoassemblies is up to $x \approx 2$ slightly blue-shifted while the intensity of the vibrational band is relatively increased [5]. This indicates that the fluorescence becomes even more forbidden which goes in line with an increase of the decay time. From this we tentatively conclude that the planarity of H_2P is enforced by the TOPO ligands upon assembly formation and the binding of 2 pyridyl groups to the QD surface. Similar effects have been reported for nanoassemblies formed from QDs and diimide dye molecules [21].

The overall conclusion from these findings is that for $x < 2$ most H_2P molecules are attached to the QD surface while the amount of free molecules is continuously increasing for $x > 2$. This is an indication that assembly formation does at least within first hours after sample preparation not follow a Poisson distribution [14, 15]. This can be seen from Figure S16 (top). However, we have shown that assembly formation is continued at a much slower formation rate at very long waiting times after the initial titration step [15].

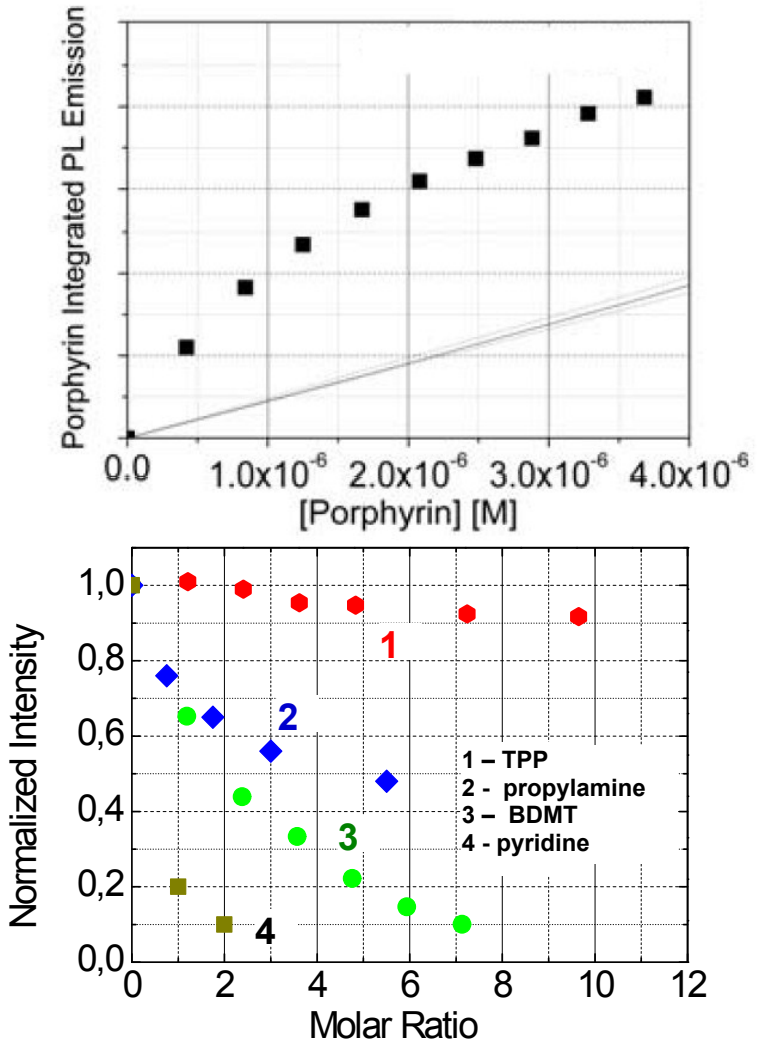

Figure S16 Top: Titration of TOPO capped CdSe(SO) by $(m\text{-}Pyr)_4H_2P$ in toluene at RT. The black line corresponds to the increase of H_2P fluorescence intensity in the absence of QDs. At the highest concentration (which corresponds to $x \approx 4$) fluorescence of H_2P is increasing with a similar slope as in the absence of QDs. This indicates that H_2P is no longer assembled with QDs or FRET has reached its maximal efficiency. **Bottom:** PL quenching upon titration of CdSe(SO) with various functionalized molecules in toluene at RT: (2) propylamine, (3) benzenedimethanethiol (BDMT) and (4) pyridine which all cause considerable PL quenching. For comparison, under the same experimental conditions and molar ratios non-functionalized porphyrin molecule (TPP) quenches QD PL only very weakly (1). In the latter case, neither the donor quenching (QD) nor the acceptor enhancement (TPP) is existent. For comparison, PL quenching by $(m\text{-}pyr)_4H_2P$ becomes ≈ 0.5 at $x = 2$ and behaves very similar to BDMT up to $x \approx 4$ and levels off for $x > 4$.

References

[1] C. Bullen, Mulvaney, P. The Effects of Chemisorption on the Luminescence of CdSe Quantum Dots. *Langmuir* (2006) **22**, 3007–3013.

[2] Ji, X.; Copenhaver, D.; Sichmeller, C.; Peng, X. Ligand Bonding and Dynamics on Colloidal Nanocrystals at Room Temperature: The Case of Alkylamines on CdSe Nanocrystals. *J. Am.*

Chem. Soc. (2008) **130**, 5726–5735.
[3] Kowerko, D.; Schuster, J.; Amecke, N.; Abdel-Mottaleb, M.; Dobrawa, R.; Würthner, F.; von Borczyskowski, C. FRET and ligand related NON-FRET processes in single quantum dot-perylene bisimide assemblies. *PhysChemChemPhys.* (2010) **12**, 4112-4123.
[4] Bowen-Katari, J. E.; Colvin, V. L.; Alivisatos A. P. X-ray Photoelectron Spectroscopy of CdSe Nanocrystals with Application to Studies of the Nanocrystal Surface. *J. Phys. Chem.* (1994) **98**, 4109-4117.
[5] E. Zenkevich, F. Cichos, A. Shulga, E. Petrov, T. Blaudeck, C. von Borczyskowski. Nanoassemblies designed from semiconductor quantum dots and molecular arrays. *J. Phys. Chem. B* (2005) **109** 8679-8692.
[6] Blaudeck, T.; Zenkevich, E. I.; Cichos, F.; von Borczyskowski, C. Probing Wave Functions at Semiconductor Quantum-Dot Surfaces by NON-FRET Photoluminescence Quenching. *J. Phys. Chem. C* (2008) **112**, 20251-20257.
[7] Knowles, K. E.; Tice, D. B.; McArthur, E. A.; Solomon, G. C.; Weiss, E. A. Chemical Control of the Photoluminescence of CdSe Quantum Dot-Organic Complexes with a Series of Para-Substituted Aniline Ligands. *J. Am. Chem. Soc*. (2010) **132**, 1041–1050.
[8] Munro, A. M.; Ginger, D. S. Photoluminescence Quenching of Single Nanocrystals by Ligand Adsorption. *Nano Lett.* (2008) **8**, 2585–2590.
[9] Moreels, I.; Martins, J. C.; Hens, Z. Ligand Adsorption/Desorption on Sterically Stabilized InP Colloidal Nanocrystals: Observation and Thermodynamic Analysis. *ChemPhysChem*. (2006) **7**, 1028–1031.
[10] Moreels, I.; Martins, J. C.; Hens, Z. Solution NMR Techniques for Investigating Colloidal Nanocrystal Ligands: A Case Study on Trioctylphosphine Oxide at InP Quantum Dots. *Sens. Actuators B.* (2007) **126**, 283–288.
[11] Chambrier I., Banerjee C., Remiro-Buenamanana S., Chao Y., Cammidge A. N., Bochmann M. Synthesis of Porphyrin−CdSe Quantum Dot Assemblies: Controlling Ligand Binding by Substituent Effects. Inorg. Chem. (2015) **54**, 7368−7380.
[12] Kilin, D. S.; Tsemekham, K.; Zenkevich, E. I.; Prezhdo, O. V.; von Borczyskowski, C., Ab Initio Study of Transfer Dynamics from a Core-Shell Semiconductor Quantum Dot to a Porphyrin Sensitizer. *J. Photochem. Photobiol. A* (2007) **190**, 342-351.
[13] G. Beane, K. Boldt, N. Kirkwood, P. Mulvaney. Energy Transfer between Quantum Dots and Conjugated Dye Molecule. *J. Phys. Chem. C* (2014) **118** 18079-18066.
[14] T. Blaudeck. Fluorescence Quenching of Semiconductor Quantum Dots by Multiple Dye Molecules, in: Self-Assembled Organic-Inorganic Nanostructures: Optics and Dynamics, 201-213 (E. Zenkevich, C. von Borczyskowski, Eds.) *Pan Stanford Publishers* (2016) Singapore.
[15] T. Blaudeck, E. I. Zenkevich, M. Abdel-Mottaleb, K. Szwaykowska, D. Kowerko, F. Cichos, C. von Borczyskowski. Formation Principles and Ligand Dynamics of Nanoassemblies of CdSe Quantum Dots and Functionalised Dye Molecules. *ChemPhysChem* (2012) **13** 959–972
[16] A. R. Clapp, I. L. Medintz, M. Mauro, M. B. R. Fisher, M. G. Bawendi M. G., H. Mattoussi. Fluorescence Resonance Energy Transfer Between Quantum Dot Donors and Dye-Labeled Protein Acceptors. *J. Am. Chem. Soc.* (2004) **126** 301–310.
[17] T. Ren, P. K. Mandal, W. Erker, Z. Liu, Y. Avlasevich, L. Puhl, K. Muellen, T. Basché. A simple and versatile route to stable quantum dot-dye hybrids in nonaqueous and aqueous solutions. *J. Am. Chem. Soc.* (2008) **130** 17242-17243
[18] G. Beane, K. Boldt, N. Kirkwood, P. Mulvaney. Energy Transfer between Quantum Dots and Conjugated Dye Molecule. *J. Phys. Chem. C* (2014) **118** 18079-18066.
[19] T. Blaudeck. Self-Assembly of Functionalized Porphyrin Molecules on Semiconductor Nanocrystal Surfaces. *PhD Thesis* (2007) TU Chemnitz.
[20] A. Ghosh. Quantum Chemical Studies of Molecular Structures and Potential Energy Surfaces of Porphyrins and Hemes, in: The Porphyrin Handbook, Vol. 7 - Theoretical and Physical Characterization, Chapter 47, p. 1-38 (K.M. Kadish, K.M. Smith, R. Guilard, Eds.) *Academic Press* (2000-2003) San Diego.
[21] D. Kowerko, S. Krause, N. Amecke, M. Abdel-Mottaleb, J. Schuster, C. von Borczyskowski. Identification of Different Donor-Acceptor Structures via FRET in Quantum-Dot-Perylene Bisimide Assemblies. *Int. J. Mol. Science* (2009) **10** 5239-5256

S9 Short Summary of PL Properties of CdSe Quantum Dots

Recently a detailed analysis of the PL emission spectra of CdSe/ZnS QDs (HY) revealed more details of the NBE PL [1-3]. Additional to the Gaussian size distribution at least 2 (Gaussian) PL bands are needed to describe the NBE PL linewidth across a temperature range from 90 to 300K. They have been tentatively assigned to PL from core and surface trap related states [2, 3]. Moreover, PL emission of shallow traps (ST) shows up energetically close to the band edge [3]. PLE spectra indicate that the PL emission of ST shows only weak size selection and is most effectively excited via elevated excitonic states (Figure S17) [3]. The distribution of energies near the band edge depends critically on the kind of ligands and attached dyes showing a strong temperature dependence of these effects [1, 3].

It is commonly reported that the PL decay of colloidal QDs is in almost all cases even under low excitation power conditions multi-exponential (see also Section S6). Analysis of the decay dynamics of NBE PL needs at RT at least 2 or 3 decay times in the range from about 1 ns to 30 ns [1-3]. (Much faster relaxation processes are observed via non-linear optical experiments and have been attributed to intra-gap relaxation and cooling of hot electrons or holes [4, 5]). IGE decays at RT within 50 ns to several μs [6]. While a distribution of PL parameters might be easily explained by inhomogeneities among QDs within an ensemble it was surprising to find that the PL of single QDs decays also multi-exponentially (besides at the highest PL intensity during a blinking time trace) in close relation with PL intensity blinking and spectral diffusion [7-9]. However, at sufficiently short observation time intervals PL of single QDs becomes mono-exponential at any PL intensity [10]. Fluctuations (blinking) in PL intensities and decay times have been assigned to charging processes [11] or interactions with multiple reaction centers [12].

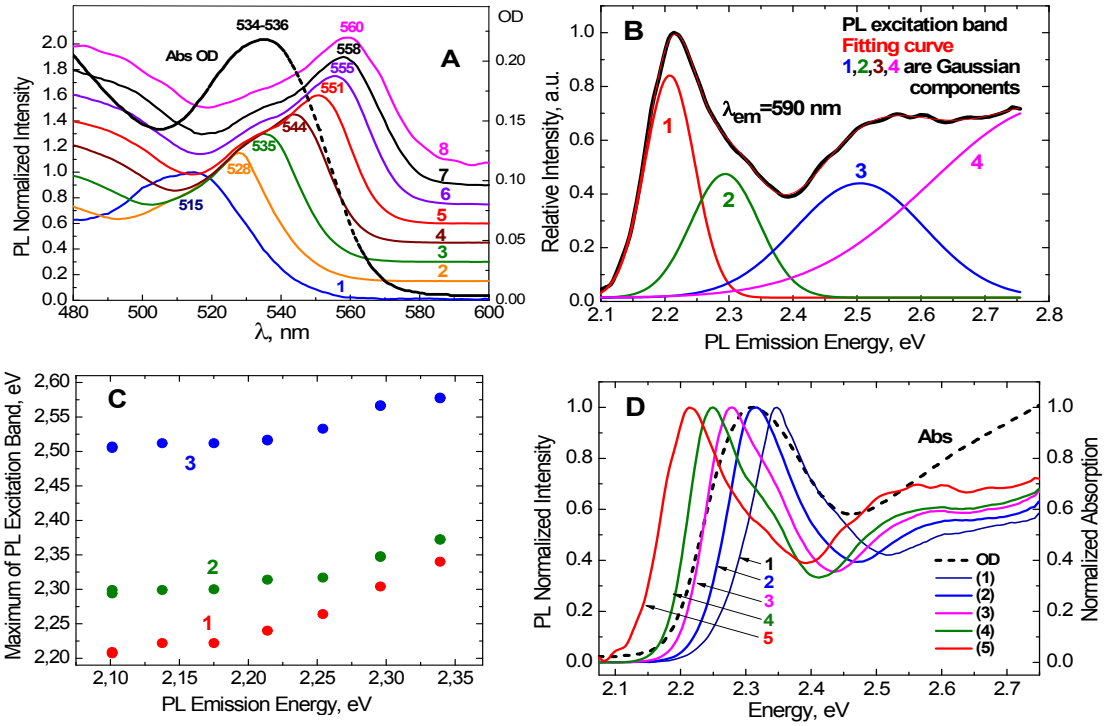

Figure S17 PL and PLE spectra with special emphasis on the spectral range of shallow traps below the band edge for TOPO capped CdSe/ZnS(HY) in toluene at RT. **A:** PL emission as a function of excitation. **B:** Deconvoluted PLE at 590 nm detection wavelength. **C:** Deconvoluted PL excitation energy versus PL emission energy. Note, that PLE energies are nearly independent of the detection wavelength below a detection energy of about 2.2 – 2.25 eV. We assign this to a decrease of the size dependence of PL. Band (1) represents a shallow trap or surface trap energetically about 100 meV below NBE states. **D:** Normalized PLE spectra as a function of detection energy: λ_{em} = 530 nm (1), λ_{em} = 540 nm (2), λ_{em} = 550 nm (3), λ_{em} = 560 nm (4), λ_{em} = 590 nm (5). Note, that the lowest detection energy (5) shows a relative increase of excitation energies at elevated energies (bands 3 and 4 in Figure S16B). The normalized absorption spectrum in the range of the first excitonic transition is shown by a dashed line. (Figure adapted from [3])

At first glance it is tempting to relate inhomogeneities within an ensemble to those of fluctuating but time-averaged single QDs. Evidence for this is provided by comparing blinking dynamics with PL photobleaching of ensembles [13-15]. However, a closer look on the dynamics as a function of NBE PL energies provides deeper insights since it has been found that PL decay times vary across the PL emission band of an ensemble. The variation is such large that it cannot be explained by the inherent size distribution and related variation of decay time [16, 17]. Strouse et al. reported for the NBE PL of CdSe QDs a (1-3) ns decay component assigned to a charged exciton red-shifted by about 20 meV from a component decaying with (20 – 30) ns (band edge exciton) [16]. They determined for QDs with variable

sizes differing radiative and non-radiative rates for the 2 identified decay components. Xiao *et al.* also found 2 decay components (2-5 and 15- 20 ns, respectively) [17]. The short component increases strongly across the NBE PL band with increasing PL energy. They tentatively assigned the long-lived component (contributing predominantly to the QY) to surface related PL. Petrov *et al.* identified for CdSe/ZnS(RQD) QDs excited resonantly into the lowest absorption band a 3-exponential decay (1ns, 10 ns and (20 – 22) ns) [18]. The fast decay contributes predominantly at high energies of the PL band but also to a much lesser content at the low energy edge of the PL band which can be seen via initial time dependent spectral red shifts (at high PL energies) and blue shifts (at low PL energies) (Fig. 6 of the respective reference [18]). In that sense their results combine the observations of Strouse *et al.* [16] and Xiao *et al.* [17].

It should be mentioned that Petrov *et al.* found also a very weak ≈ (50 – 100) ns decay at the very red edge of the NBE PL [18, 20]. Similar results have been reported previously for CdSe/ZnS(HY) [1, 11] and are shown also for CdSe(SO) in Figure S14.

How do these results - which are qualitatively in accordance with each other though obtained for different kinds of CdSe QD ensembles - compare with single QD data? Recently we have shown that intermittent PL intensities of a single QD are uniquely related with fluctuations in PL decay times and PL energies: short decay times (that is low PL intensities) correspond with low PL energies [1, 9, 11]. At first glance the finding of short decay times predominantly at low PL energies seems to be in contradiction to what has been observed in the majority of ensemble experiments, namely short decay times both at high and to a less extent at low energies. In principle, the apparent contradiction between ensemble and single QD experiments can be solved remembering that ensemble experiments cover inhomogeneities of QD properties. We assume that a certain fraction of QDs, namely those, which are during most of the observation time characterized all the time by a very short and thus basically non-radiative decay, is mostly missed in single QD experiments since such single QDs will be not identified according to their low QY.

But why should such heavily quenched QDs be observed systematically more often in the high energy range of the NBE PL? Such a systematic dependence has been explained previously by Rogach *et al*. as being due to the consequences of Oswald ripening [20]. To understand their findings, we have to remember that the width of a PL band is governed by the size distribution remaining in an ensemble after chemical synthesis. During this synthesis the QDs finally found in the centre of the PL band are those which grew in a dynamic equilibrium during the ripening process while the growing dynamics heavily deviate from

equilibrium for smaller sized QDs (typically observed at high PL energies). Deviation from a growing process in dynamic equilibrium results in an increase of surface defects and is responsible for fast non-radiative trapping of excitons [20]. Inhomogeneous distributions of surface trapping of excitons have already been identified earlier [21] for ensembles of CdSe QDs. Obviously, single QD detection misses fast decaying QDs in the high NBE energy range due to their extremely low QY but can identify those QDs intermittent between high and low QYs. The latter are due to the quantized Stark effect red-shifted to low PL energies by (20 – 50) meV [9, 11]. The essential conclusion is (see Scheme in Figure S15) that an ensemble of QDs is subject to both a (static) distribution of QDs with a systematically distributed large range of PL QYs and to intermittency of (probably) all QDs. On the other hand, single QD detection misses in most cases those QDs (in this case at the high energy range of the PL band) with extremely low QYs [22].

How do these findings correspond with the PL quenching upon assembly formation with H_2P-type molecules? We found that the ratio between slow and fast decaying components is at 290 K without any significant PL energy related dependence increased considerably in favor of the shortest one [1, 2]. From this we conclude that PL quenching is related to both increase of the (*i*) concentration of quenching surface traps in the high energy range (also detected by ensemble experiments on QDs without attached dyes) and (*ii*) intermittent "charged" states detected by ensemble and single QD experiments in the low energy range of PL.

The situation is somewhat different at 77 K at which we did not find a 1 ns component at the low energy side of the PL band of CdSe/ZnS which implies that surface related defects are only present in the high energy range [3]. (The difference between low and high temperature results has been explained by an intermediate phase transition of ligands [1, 2, 23].) We observed a kind of phase transition of ligands at about 230 K which results at 77 K in the formation of a series of trap states shifted below the NBE PL. We found that all PL decay times are noticeably shortened below the phase transition temperature [1, 2]. Again, we observe an overall in-growth of the fast decay component upon assembly formation which is now distributed like at RT across the total PL band [1, 2]. The ratio of the fast to slow components at high or respectively low PL energy is increased most significantly for CdSe/ZnS-CuP nanoassemblies (containing tetrapyridyl substituted Cu-porphyrin) which we ascribed to the in comparison to CdSe/ZnS-H_2P nanoassemblies more strongly induced depletion of TOPO ligands by TOPO-complexing CuP [2, 23].

The blue-shifted and short decay NBE component is (at 77 K) enhanced with increasing

polarity of the solvent which we take as an indication that charging is involved with this component similar to findings obtained for blinking processes [11, 15, 24-26]. However, long lived PL exciton decay times do not depend substantially on solvent polarity at a given temperature but the switching time among different PL intensities with inherently related shortened decay times is further considerably shortened with increasing ε [9]. Qualitatively similar results with respect to the relation of PL energy and QY have been reported by Kowerko *et al.* also showing that attachment of perylene diimide molecules enhances considerably the bluing of CdSe/ZnS QDs with amine ligands [27]. Polarity effects on PL of single QDs have also been reported elsewhere [28, 29]

We note similar to reported results [30, 31] that the with respect to NBE PL red-shifted IGE is considerably increased with decreasing temperature. Figure S18 shows the temperature dependent luminescence of CdSe/ZnS(HY)-CuP nanoassemblies at x = 1. We have chosen this dye since CuP does not have significant fluorescence in the range of IGE close to 650 nm [1, 2]. Besides the PL of CdSe PL a strongly temperature dependent luminescence is observed for λ > 600 nm which can be deconvoluted into 3 bands (see Figure S18). Part of this broad emission is assigned to the phosphorescence from the CuP triplet state in the range of 750 – 785 nm [2]. We assign the other 2 bands (curves 2 and 3) to IGE PL of CdSe/ZnS. At least the band at (650 – 680 nm) shows a phase transition-type sudden intensity change at about 220 K which has been assigned previously to a phase transition of the TOPO ligand shell causing a re-ordering of trap and intra-gap states [1, 2, 23].

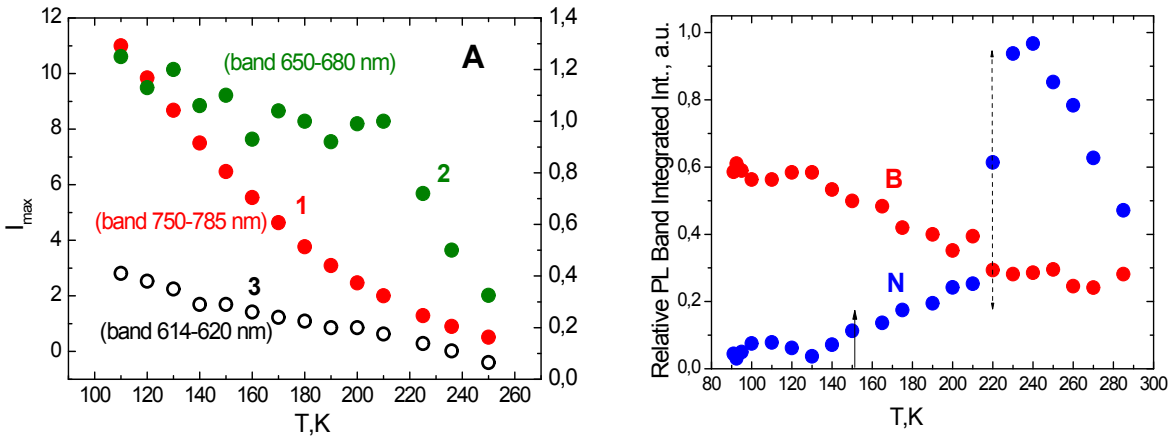

Figure S18 Temperature dependent PL of CdSe/ZnS(HY)-CuP nanoassemblies (x = 1) in methylcyclohexane-toluene (6:1) mixture at λ_{exc} = 450 nm. **Left**: Temperature dependence of PL intensities of 3 deconvoluted spectral bands (1: left scale; 2, 3: right scale) in the IGE spectral range of CdSe/ZnS-CuP nanoassemblies (x = 1). The (720 – 785 nm) band (red points 1, left scale) is mainly due to the phosphorescence of the CuP triplet state. **Right**: Temperature dependence in the NBE spectral range (relative integrated PL band intensities of spectral bands). Fits have been performed

with two Gaussian components, termed B (broad) and N (narrow). The temperature T_{crit} (≈ 220 K) of a phase transition of the capping TOPO layer is indicated by the dashed arrow. The glass transition temperature is at 151.6 K for a methylcyclohexane/toluene (6:1) mixture and indicated by a solid arrow [1].

The intensity of this band increases with decreasing temperature below the phase transition temperature. This is opposite with to what is observed for the NBE PL of CdSe/ZnS(HY)-CuP nanoassemblies which show a very strong decrease of PL intensity below phase transition temperature [1, 2]. Such an observation is in agreement with the temperature dependence reported for IGE [30, 31]. The IGE band at (614-620 nm) is in the range of shallow trap emission and shows a similar behavior as the (650-680 nm) band which implies that shallow traps are more effectively generated and/or populated with decreasing temperature.

Finally, Figure S19 shows a comparison of PLE spectra for CdSe/ZnS(HY) QDs in toluene at 293 K at 2 detection wavelengths including IGE.

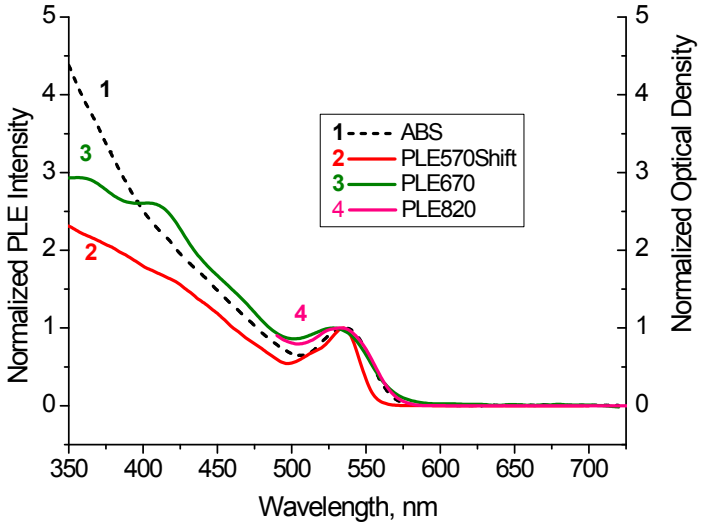

Figure S19 Comparison of absorption and PLE spectra for CdSe/ZnS(HY) QDs in toluene at 293 K for 3 detection wavelengths at λ_{det} = 570 nm (shifted to the absorption band maximum), 670 nm and 820 nm, respectively.

The results are similar to those of CdSe/ZnS(LPB), CdSe/ZnS(CG) and CdSe(SO) in Figures S9, S10 and S6, respectively. In comparison with absorption all normalized PLE spectra have in common (see also [11]) that NBE PL is relatively small at elevated excitation energies while IGE gets relatively enhanced across the comparable high energy range. Only PLE of CdSe(SO) shows an enhanced PLE range below NBE excitation as compared to absorption. Notably, at excitation wavelengths below ≈ 400 nm PLE of IGE drops below the absorption curve. This can be interpreted by the fact that excitation above a certain energy

does not result in any detectable IGE but is either followed by the formation of completely radiationless states or a very fast deactivation to lower exciton states circumventing IG state formation. The latter assumption is supported by the observation that PLE of NBE PL does not show such a bending of the PLE curve above a certain energy [32].

References

[1] E. I. Zenkevich, A. Stupak, D. Kowerko, C. von Borczyskowski. Influence of single dye molecules on temperature and time dependent optical properties of CdSe/ZnS quantum dots: Ensemble and single nanoassembly detection. *Chem. Phys.* (2012) **406** 21 – 29.

[2] E. Zenkevich, A. Stupak, C. Goehler, C. Krasselt, C. von Borczyskowski. Tuning Electronic States of a CdSe/ZnS Quantum Dot by Only One Functional Dye Molecule. *ACS Nano* (2015) **9** 2886-2907.

[3] E. Zenkevich, A. Stupak, C. von Borczyskowski. New Insights: Photophysics of CdSe Quantum Dots - A Temperature Related Approach, in: Tuning Semiconducting and Metallic Quantum Dots: Spectroscopy and Dynamics, p. 41- 102, C. von Borczyskowski, E. Zenkevich (Eds.) *Pan Stanford Publishing* (2016) Singapore.

[4] V. Klimov, P. Haring Bolivar, H. Kurz. Ultrafast carrier dynamics in semiconductor quantum dots. *Phys. Rev. B* (1996) **53** 1463.

[5] C. Burda, T. C. Green , S. Link, M. A. El-Sayed. Electron Shuttling Across the Interface of CdSe Nanoparticles Monitored by Femtosecond Laser Spectroscopy. *J. Phys. Chem. B* (1999) **103** 1783–1788.

[6] C. Burda, S. Link, M. Mohamed, M El-Sayed. The Relaxation Pathways of CdSe Nanoparticles Monitored with Femtosecond Time-Resolution from the Visible to the IR: Assignment of the Transient Features by Carrier Quenching. *J. Phys. Chem. B* (2001) **105** 12286–12292.

[7] G. Schlegel, J. Bohnenberger, I. Potapova, A. Mews. Fluorescence decay time of single semiconductor nanocrystals. *Phys. Rev. Lett.* (2002) **88** 137401.

[8] B. R. Fisher, H.-J. Eisler, N. E. Stott, M. G. Bawendi. Emission Intensity Dependence and Single-Exponential Behavior in Single Colloidal Quantum Dot Fluorescence Lifetimes. *J. Phys. Chem. B* (2004) **108**143–148.

[9] R. Schmidt, C. Krasselt, C. Göhler, C. von Borczyskowski. The Fluorescence Intermittency for Quantum Dot Is Not Power-Law Distributed: A Luminescence Intensity Resolved Approach. *ACS Nano* (2014) **8** 3506-3521.

[10] J. Cui, A. P. Beyler, T S. Bischof, M. W. B. Wilson, M. G. Bawendi. Deconstructing the photon stream from single nanocrystals: from binning to correlation. *Chem. Soc. Rev.* (2014) **43** 1287-1310.

[11] I. Trenkmann, C. Göhler, C. Krasselt, C. von Borczyskowski. Tuning Luminescence Intermittency, in: Tuning Semiconducting and Metallic Quantum Dots: Spectroscopy and Dynamics, p. 283-376, C. von Borczyskowski, E. Zenkevich (Eds.) *Pan Stanford Publishers* (2016) Singapore.

[12] P. A. Frantsuzov, S. Volkán-Kacsó, B. Jankó. Universality of the Fluorescence Intermittency in Nanoscale Systems: Experiment and Theory. *Nano Lett.* (2013) **13** 402–408.

[13] I. Chung, M. G. Bawendi. Relationship between single quantum-dot intermittency and fluorescence intensity decays from collections of dots. *Phys. Rev. B* (2004) **70** 165304.

[14] F. Cichos, J. Martin, C. von Borczyskowski. Emission intermittency in silicon nanocrystals. *Phys. Rev. B* (2004) **70** 1153141.

[15] F. Cichos, C. von Borczyskowski, M. Orrit. Power-law intermittency of single emitters. *Curr. Op. Coll. Interf. Science* (2007) **12** 272-284.

[16] A. Javier, D. Magana, T. Jennings, F. Strouse. Nanosecond exciton recombination dynamics in colloidal CdSe quantum dots under ambient condition. *Appl. Phys. Lett.* (2003) **8** 1423-1425.

[17] X. Wang, L. Qu, J. Zhang, X. Peng, M. Xiao. Surface-Related Emission in Highly Luminescent CdSe Quantum Dots. *Nano Lett (*2003) **3** 1103-1106.

[18] E. P. Petrov, F. Cichos, C. von Borczyskowski. Intrinsic photophysics of semiconductor nanocrystals in dielectric media: Formation of surface states. *J. Luminesc.* (2006) **119-120** 412-

417.
[19] E. Zenkevich, F. Cichos, A. Shulga, E. Petrov, T. Blaudeck, C. von Borczyskowski. Nanoassemblies designed from semiconductor quantum dots and molecular arrays. *J. Phys. Chem. B* (2005) **109** 8679-8692.
[20] A. L. Rogach, T. Franzl, T. A. Klar, J. Feldmann, N. Gaponik, V. Lesnyak, A. Shavel, A. Eychmueller, Y. P. Rakovich, J. F. Donegan. Aqueous Synthesis of Thiol-Capped CdTe Nanocrystals: State-of-the-Art. *J. Phys. Chem. C* (2007) **111** 14628-14637.
[21] R. A. Jense, I. C. Huang, O. Chen, J. T. Choy, T. S. Bischof, M. Lonca, M. G. Bawendi. Optical Trapping and Two-Photon Excitation of Colloidal Quantum Dots Using Bowtie Apertures. *ACS Photonics* (2016) **3** 423-427.
[22] S. F. Lee, M. A. Osborne. Photodynamics of a Single Quantum Dot: Fluorescence Activation, Enhancement, Intermittency, and Decay. *J. Am. Chem. Soc.* (2007) **129** 8936–8937.
[23] E. Zenkevich, C. von Borczyskowski. Structural and Energetic Dynamics in Quantum Dot- Dye Nanoassemblies, in: Self-Assembled Organic-Inorganic Nanostructures: Optics and Dynamics, p. 1-147, E. Zenkevich, C. von Borczyskowski (Eds.) *Pan Stanford Publishers* (2016) Singapore.
[24] A. Issac, C. von Borczyskowski, F. Cichos. Correlation between photoluminescence intermittency of CdSe quantum dots and self-trapped states in dielectric media. *Phys. Rev. B* (2005) **71** 161302.
[25] A. Issac, C. Krasselt, F. Cichos, C. von Borczyskowski. Influence of the Dielectric Environment on the Photoluminescence Intermittency of CdSe Quantum Dots. *ChemPhysChem* (2012) **13** 3223–3230.
[26] C. von Borczyskowski, E. Zenkevich. Formation Principles and Exciton Relaxation in SemiconductorQuantum Dot-Dye Nanoassemblies, in: Quantum Dot Molecules, Lecture Notes in Nanoscale Science and Technology, p. 77-148, J. Wu, Z. M. Wang (Eds.) *Springer* (2014) New York, Heidelberg, Dordrecht, London.
[27] D. Kowerko. Interrelation of Assembly Formation and Ligand Depletion in Colloidal Quantum Dots, in: Self-Assembled Organic-Inorganic Nanostructures: Optics and Dynamics, 149-200, E. Zenkevich, C. von Borczyskowski (Eds.) *Pan Stanford Publishers* (2016) Singapore.
[28] D. E. Gomez, J. van Embden, P. Mulvaney. Spectral diffusion of single semiconductor nanocrystals: The influence of the dielectric environment. *Appl. Phys. Lett*. (2006) **88** 154106.
[29] S. F. Lee, M. A. Osborne. Brightening, blinking, bluing and bleaching in the life of a quantum dot: friend or foe? *ChemPhysChem* (2009) **10** 2174-2191.
[30] P. Nemec, P. Malý. Temperature Study of Trap-related Photoluminescence Decay in CdS_xSe_{1-x} nanocrystals in Glass. *J. Appl. Phys.* (2000) **87** 3342-3348.
[31] J. Mooney, M. M. Krause, J. I. Saari, P. Kambhampati. A microscopic picture of surface charge trapping in semiconductor nanocrystals. *J. Chem. Phys.* (2013) **138** 204705.
[32] W. Hoheisel, V. L. Colin, C. S. Johnson, A. P. Alivisatos. Threshold for quasicontinuum absorption and related luminescence efficiency in CdSe nanocrystals. *J. Chem. Phys.* (1994) **101** 8455-8460.